Mangino, G.; Vilanova Navarro, S.; Plazas Ávila, MDLO.; Prohens Tomás, J.; Gramazio, P. (2021). Fruit shape morphometric analysis and QTL detection in a set of eggplant introgression lines. Scientia Horticulturae. 282:1-14. https://doi.org/10.1016/j.scienta.2021.110006

Fruit shape morphometric analysis and QTL detection in a set of eggplant introgression lines

Giulio Mangino[a], Santiago Vilanova[a], Mariola Plazas[b], Jaime Prohens[a] and Pietro Gramazio[c,*]

Affiliations

[a]*Instituto de Conservación y Mejora de la Agrodiversidad Valenciana, Universitat Politècnica de València, Camino de Vera 14, 46022 Valencia, Spain*

[b]*Meridiem Seeds S.L., Paraje Lo Soler 2, 30700 Torre-Pacheco, Spain*

[c]*Faculty of Life and Environmental Sciences, University of Tsukuba, 1-1-1 Tennodai, 305-8572, Tsukuba, Japan*

[*] Corresponding author

Pietro Gramazio: gramazio.pietro.gn@u.tsukuba.ac.jp

Abstract

Eggplant fruit shape is an important quantitative agronomic trait. The use of introgression lines (ILs) for QTLs identification is a powerful tool for the elucidation of the genetic control of eggplant fruit shape. In the present study, a set of 16 eggplant ILs, each harboring a single marker-defined chromosomal segment from the wild eggplant relative *S. incanum* in the genetic background of *S. melongena*, was evaluated for fruit shape in two environments (open field and screenhouse). A detailed phenotyping of the fruits of the two parents, hybrid and ILs was performed using 32 morphological descriptors of the phenomics tool Tomato Analyzer. Several morphological differences were found between parents, and the hybrid displayed negative heterosis for many fruit shape traits, being more similar to the *S. incanum* parent. Significant differences for most fruit shape descriptors were found between ILs and the recipient parent. For many descriptors, the genotype factor had the highest contribution to the percentage of the sum of squares. Although the contributions of the environment and the G × E interaction were significant for almost all descriptors, their effects on fruit shape were relatively low. Hierarchical clustering revealed nine clusters of highly correlated traits and six ILs groups. A total of 41 stable QTLs spread over ten chromosomes were detected. Of these, twenty QTLs associated to Basic Measurement and Fruit Shape Index descriptors were syntenic to other previously reported in several intraspecific and interspecific eggplant populations, while twenty-one QTLs, including Blockiness, Homogeneity, Asymmetry and Internal Eccentricity, were new. In addition, mutations associated to genes belonging to *SUN*, *OVATE* and *YABBY* families described in tomato were reported in the QTLs genomic regions identified in eggplant. Eleven *SUN* and *YABBY* genes were proposed as potential candidate controlling fruit shape variations in eggplant. Our results provide novel and highly relevant insights on the genetics of fruit shape in eggplant and have important implications for eggplant breeding.

Keywords: *Solanum melongena*, *S. incanum*, introgression lines, fruit shape, morphometric analysis, Tomato analyzer, QTLs

1. Introduction

Fruit shape is a trait of great agronomic and commercial relevance in many vegetable crops grown for this organ (Snouffer et al., 2020). Although fruit shape can be affected by the environment, it is largely genetically determined (Wu et al., 2018; Pan et al., 2020). Together with fruit size, fruit shape was among the major traits under selection during the domestication of fruit-bearing crops, resulting in a broad diversity of fruit shapes in most of these cultivated species. In this way, in tomato, starting from small rounded fruits typical of wild relatives, the domestication process led to a gradual selection and accumulation of mutations associated with larger size and diverse shapes, giving rise to a wide variability of combinations of fruit shape and size of present-day cultivars (Tanksley, 2004; Klee and Resende, 2020; Mata-Nicolás et al., 2020).

The accurate study of the fruit shape requires objective and precise phenotypic analysis, requiring a detailed set of morphological descriptors (Brewer et al., 2006). However, fruit shape is frequently evaluated by measuring simple traits, like fruit length and width, and by identifying shape patterns that could be matched with qualitative descriptors (IPGRI, 1996; Scott, 2010; UPOV, 2013). Although these traits provide relevant information and are easily measurable, they do not allow a detailed characterization of the fruit shape (Costa et al., 2011). With the development of modern phenomics tools, many additional fruit shape features, which are often difficult to score by hand, can be accurately measured, providing a more precise and comprehensive characterization of fruit morphology. In this respect, a free software tool, Tomato Analyzer, allows phenomics studies of tomato fruit shape through high-throughput quantitative measurements of many fruit traits from scanned images of fruit sections (Brewer et al. 2007; Gonzalo and van der Knaap 2008; Rodríguez et al. 2010a, 2010b). Although Tomato Analyzer has proven to be very useful for morphological and morphometric characterization of tomato fruit (Rodríguez et al., 2011, 2013; Figas et al., 2015; Nankar et al.,

2020), it has also been successfully used for the characterization of other vegetable crops like eggplant (Hurtado et al., 2013), melon (Diaz et al., 2017; Oren et al., 2020), or pepper (Tripodi and Greco, 2018; Pereira-Diaz et al., 2020).

Over the past decades, different segregating populations have been used for dissecting quantitative trait loci (QTL) of physiological and agricultural interest in plants. In particular, F2 populations or recombinant inbred lines (RILs), which are easier to develop, have allowed the detection of numerous QTLs (Nadeem et al., 2018). On the other hand, introgression line (IL) populations, a set of fixed and immortal lines that cover the totality or part of a donor parent genome carrying one or a few introgressed fragments into the genetic background of a recipient parent, allow a more efficient and precise identification of QTLs compared to other segregating populations like F2 and RILs (Yin et al., 2016; Fasahat et al., 2016; Boopathi, 2020). In IL populations, linkage drag is reduced by the small portion of introgressed donor genome of the lines, and, therefore, the phenotypic variation between ILs can be accurately attributed to specific introduced segments (Zamir, 2001). Once a QTL associated with a trait of interest is localized, this information can be used for a better estimation of gene × gene (epistasis) and gene × environment (G x E) interactions, pleiotropic effects, and mapping strong QTL effects (Gur and Zamir, 2015; Balakrishnan et al., 2019). Furthermore, each IL can be used as a starting point for developing lines with smaller introgression (sub-ILs) for increased mapping resolution (Monforte and Tanksley, 2000; Chakrabarti et al., 2013; Sacco et al., 2013) and performing QTL positional cloning (Salvi and Tuberosa, 2005). However, the major limitation of using IL populations for quantitative studies is the investment in time and resources required to develop them (Yan et al., 2017; Can et al., 2019; Alqudah et al., 2020).

Tomato (*Solanum lycopersicum* L.) is the model system to study fruit shape in Solanaceae, and specifically for fleshy-fruited plant species, with many studies that have allowed identifying the major “domestication” genes controlling the wide phenotypic diversity of the tomato fruit

(Kimura and Sinha, 2008; Kim et al., 2017; Anwar et al., 2019). Numerous QTL mapping studies for dissecting the genetic base of fruit shape have been conducted in tomato using inter-specific F2 populations obtained by crossing the cultivated tomato and different small-fruited wild species (Eshed and Zamir, 1995; Bernacchi et al., 1998; Lippman and Tanksley, 2001; van der Knapp et al., 2003; Frary et al., 2004). Additional mapping experiments have been performed using complete IL libraries (Barrantes et al., 2016; Celik et al., 2017; Di Giacomo et al., 2020) or reduced set of ILs covering specific QTL regions of different chromosomes (Monforte et al., 2001; Yates et al., 2004; Haggard et al., 2013). In this way, numerous QTLs and/or genes involved in the genetic regulation of fruit morphology in tomato have been identified. Among the major genes controlling variation in tomato fruit shape, *SUN* and *OVATE* control fruit elongation, while *FASCIATED* (*FAS*) control locule number (van der Knaap and Ostergaard, 2018). *SUN*, *OVATE* and *FAS* have been identified by positional cloning and encode a member of IQ Domain, Ovate Family Protein (OFP) families, and YABBY family, respectively (Liu et al., 2002; Xiao et al., 2008; Cong et al., 2008).

In eggplant (*Solanum melongena* L.), fruit shape is also a relevant attribute that determines its commercial use and economic value. Eggplant fruits are fleshy berries commercially classified according to their shape. As occurs with tomato (Paran and van der Knaap, 2007; Mata-Nicolás et al., 2020), a wide diversity exists for fruit shape in eggplant (Daunay et al., 2008; Wang et al., 2008; Hurtado et al., 2012), and small differences in fruit shape may be determinant for the success or failure of a commercial cultivar. The knowledge of the genetic base of fruit shape in eggplant is limited to findings obtained from QTL mapping analysis in a few biparental populations (Doganlar et al., 2002; Frary et al., 2014; Portis et al., 2014; Wei et al., 2020) and GWAS studies (Portis et al., 2015), which identified some major QTLs associated to simple fruit shape traits. Although phenomics studies utilizing Tomato Analyzer have been performed in eggplant using different eggplant germplasm materials (Prohens et al., 2012; Hurtado et al.,

2013; Plazas et al., 2014; Kaushik et al., 2016, 2018), their aim was describing the diversity in collections of materials and segregating populations and not associating genomic regions with underlying genes controlling natural variations of fruit shape.

In this work, we analyze the fruit shape in a collection of eggplant ILs with introgressions from a wild species (*S. incanum* L.) in two different environments (open field and screenhouse) and perform a detailed phenotyping using the Tomato Analyzer tool. Stable QTLs and potential candidate genes are identified in the introgressed genomic regions. The obtained results provide novel and highly relevant insights on the genetics of fruit shape in eggplant and represent a step forward in the understanding of this trait of great interest for eggplant breeding.

2. Materials and methods

2.1. Plant material and cultivation conditions

From the IL population of *Solanum incanum* (MM577) developed in the *S. melongena* (AN-S-26) background (Gramazio et al., 2017), a set of 16 ILs were selected based on a maximization of representation of the genome of *S. incanum* and on seed availability. Characteristics of the parents and statistics of ILs set, which overall cover 58.6% of the genome of the wild *S. incanum* and for some chromosomes include overlapping ILs, are described in detail in Mangino et al. (2020). Seed germination was performed using the protocol described in Ranil et al. (2015), which is suitable for wild and wild-derived materials, and seedlings were maintained in a climatic chamber with 16 h light (25 °C) / 8 h dark (18 °C) regime. Five replicates, each one consisting of a plant, for each of the two parents, the F1 hybrid, and the 16 ILs were grown under two different conditions (open field and screenhouse) during the spring-summer season of 2017 at the campus of Universitat Politècnica de València (GPS coordinates: latitude, 39° 28’ 55” N; longitude, 0°20’ 11” W; altitude 7 m a.s.l) using the standard

horticultural practices. Plants were spaced 1.5 m between the rows and 1.2 m within the rows and distributed according to a completely randomized block-design with five blocks per condition. Irrigation and fertilization were applied with a drip irrigation system. Weeds were removed manually and phytosanitary treatments against spider mites and whiteflies were performed when necessary.

2.2. Tomato Analyzer characterization

At the commercially ripe stage, three fruits per replicate were harvested, cut longitudinally and scanned with a Plustek OpticSlim 1180 (Plustek, Taipei, Taiwan) image scanner at a resolution of 300 dpi (Figure 1). Image data were subjected to a morphometric analysis with Tomato Analyzer v 3.0 software (Rodríguez et al., 2010a). A total of 32 morphological descriptors, categorized into basic measurements (7), fruit shape index (3), blockiness (3), homogeneity (3), proximal fruit end shape (3), distal fruit end shape (2), asymmetry (6), and internal eccentricity (5), were automatically recorded. Manual adjustments were done when the software was unable to accurately identify the outline of a trait. A brief description of each trait, their acronyms and evaluation methodology are described in Table 1 and visualized in Figure 2. A more detailed description of each descriptor is available at the Tomato Analyzer software webpage (https://vanderknaaplab.uga.edu/tomato_analyzer.html).

2.3. Data analysis

For each trait, means, standard errors and range values were calculated for each parent and F1 hybrid in both environments. Mid-parent heterosis values (H_{MP}) were calculated as:

$$H_{MP} = (F1-MP)/MP$$

where *F1* is the performance of the F1 hybrid and *MP* is the mean value of the parents. Statistical significance of heterosis, as well as statistically significant differences between parents for each environment, were detected using Student's *t*-tests at $p < 0.05$.

To evaluate the difference among ILs and the cultivated parent AN-S-26, data for all morphological traits were subjected to a two-factorial (genotype and environment) analysis of variance (ANOVA) including the interaction among both main factors. The total sum of squares was partitioned into sums of squares for genotype, environment, genotype × environments (G × E), block and residual effect, and expressed in percentage over total sums of squares. A fixed effects model was used for genotype and environment effect. All statistics were conducted using the Statgraphics Centurion XVII software (Statpoint Technologies, Warrenton, USA).

Pearson linear correlation (*r*) among morphological descriptors were studied. A hierarchical clustering heatmap displaying numeric differences for morphological descriptors across ILs and AN-S-26 parent in the two environments was performed using Clustvis (Metsalu and Vilo, 2015; http://biit.cs.ut.ee/clustvis/) with log-transformed data. Both rows and columns were clustered using correlation distance and average linkage.

2.4. QTL detection

For non-overlapping ILs, QTLs detection was performed by carrying out a Dunnett's test to compare the means of each IL, in the open field or screenhouse, with the recipient parent AN-S-26 (SM). For overlapping ILs a system of linear equations was used to assign a mean value to each of the introgressed genomic fragments in which the overlapping lines could be divided and *t* values for each of the introgressed genomic fragments were calculated according to the Dunnett's test procedure. A stable QTL was only reported for the non-overlapping ILs or for the introgressed genomic fragments in the overlapping ILs if the Dunnett's test was significant

($p < 0.05$) and of the same nature (i.e., either positive or negative) in both environments. The relative increase over the recipient parent and allelic effects in each of the environments were estimated as:

$$\text{Increase over recurrent parent (\%)} = (D/SM) \times 100$$

$$\text{Allelic effect} = D/2$$

Where SM is the average value for the recurrent *S. melongena* parent AN-S-26 parent and D is the difference between the mean of the IL and AN-S-26 for non-overlapping lines or the calculated difference over the mean of AN-S-26 caused by the introgressed genomic fragments in the case of overlapping lines.

2.5. Analysis of orthologous shape genes located within QTL regions

In order to detect putative eggplant orthologous of tomato genes controlling fruit shape and determine their physical location on QTL region, the cDNA sequences of 74 genes belonging to SUN, OVATE and YABBY gene family described in Huang et al. (2013) were retrieved from the Heinz 1706 tomato reference genome (version SL4.0) in the Sol Genomics Network database (http://www.solgenomics.net). Tomato cDNA sequences were blasted against the 67/3 eggplant reference genome (version V3) database (http://www.eggplantgenome.org), and information regarding orthologous eggplant genes as well as their sequence and physical location on respective chromosomes were obtained. Individual VCF file of parents (Gramazio et al., 2019), including variant effects predicted according to SnpEff software v 4.2 (Cingolani et al. 2012), were filtered out for selecting allelic variants of the identified orthologous genes. Homozygous allelic variants characterized by amino acid substitution or indel between the two parents and classified by high/moderate impact were submitted to SIFT (Sorting Intolerant From Tolerant) (Ng and Henikoff, 2001) and PROVEAN (PROtein Variation Effect Analyzer)

(Choi et al., 2012) software in order to predict significant impacts on protein functionality, using a threshold of 0.05 in SIFT and -2.5 in PROVEAN, respectively.

3. Results

3.1. Parents fruit characterization and heterosis

For the recipient parent AN-S-26, significant differences ($p < 0.05$) between the two environments were found only for Ellipsoid, Circular and Asv fruit shape descriptors (Table 2). Since MM557 and the hybrid did not set fruit in the screenhouse, the estimation of significant differences between parents as well as mid-parent heterosis under screenhouse conditions was not possible. Eggplant wild relatives and interspecific hybrids often have specific environmental and weather requirements for each plant stage like germination, vegetative development, and fruit set, which are frequently unsynchronized and different to those of the cultivated eggplant. Furthermore, these differences are wider under protected conditions, like the ones under a screenhouse. Significant differences ($p < 0.05$) between the recipient parent AN-S-26 and the donor parent MM557 were found for 24 out of 32 descriptors in the open field. Descriptors for which no significant differences were found were P_Blockiness, D_A_Micro, D_A_Macro, Ovoid, Asov, Eccentricity, P_Eccentricity and D_Eccentricity (Table 2). Compared to AN-S-26, in the open field MM557 exhibited lower values for 21 traits, except for Triangle, PA_Micro and PA_Macro (Table 2).

In the open field, the hybrid displayed significant negative values of heterosis over the mid-parent for three descriptors of Fruit Shape Index (Fruit_Shape_E_I, Fruit_Shape_E_II, C_F_Shape), two of Homogeneity (Ellipsoid, Circular), three of Asymmetry (Obovoid, Asob, Width_WP), and two of Internal Eccentricity (P_Eccentricity and F_Shape_I), ranging from -

0.002 (P_Eccentricity) to -0.573 (Asob) (Table 2). Significant positive values of heterosis were detected only for PA_Micro (0.093).

3.2. Analysis of variance

For all the descriptors, the ANOVA revealed that the differences among the ILs and the *S. melongena* parent were statistically significant ($p < 0.05$) for at least one of the factors (genotype, environment and genotype × environment) for all fruit shape descriptors, with the exception of PA_Micro, DA_Macro, Asv, P_Eccentridicty and D_Eccentricity (Table 3 and Figure 2). Important differences between genotypes were found, with significant ($p < 0.05$ or $p < 0.01$) or highly significant ($p < 0.001$) differences for 4 and 23 descriptors, respectively. The contribution of the genotype factor to the total sums of squares ranged from 16.6% (DA_Micro) to 49.08% (F_Shape_E_I). Moreover, the genotype factor was the greatest contributor to the sums of squares for 14 descriptors (>30%), of which three corresponded to descriptors related to Basic Measurements (Height_MW, Max_Height, and C_Height), three to Fruit Shape Index (F_Shape_E_I, F_Shape_E_II and C_F_Shape), three to Blockiness (P_Blockiness, D_Blockiness and Triangle), two to Homogeneity (Ellipsoid and Circular), one to Proximal Fruit End Shape (PA_Macro), and two to Internal Eccentricity (F_Shape_I and Ec_Area) (Table 3).

Significant differences between environments were detected for all the descriptors, except for Sh_Height. With a contribution ranging from 1.75% to 20.9% to the total sums of squares, the environmental factor was not the main contributor to the sums of squares for any of the fruit shape descriptors evaluated (Table 3).

The G × E interaction was statistically significant for all descriptors, except for P_Blockiness, Triangle, Asob and Eccentricity. The G × E contribution to the total sums of squares, which ranged from 10.2% to 24.4% exceed that of the environment contribution for all traits, except

297 for the seven Basic Measurements descriptors (Perimeter, Area, Width_MH, Max_Width,
298 Height_MW, Max_Height and C_Height). Nevertheless, as for the environment, the interaction
299 did not represent the predominant contributor to the total sums of squares for any of the
300 evaluated descriptors (Table 3).
301 The residual effect had a contribution to the total sums of squares ranging between 28.89% and
302 61.14% and was the greatest contributor to the total sums of squares for 13 descriptors, of
303 which four corresponded to Basic Measurement descriptors (Perimeter, Area, Width_MH and
304 Max_width), one to Homogeneity (Rectangular), one to Proximal Fruit End Shape
305 (Sh_Height), one to Distal Fruit End Shape (DA_Micro), five to Asymmetry (Obovoid, Ovoid,
306 Asob, Asov and Width_WP), and one to ~~was~~ Internal Eccentricity (Eccentricity) (Table 3).
307
308 *3.3. Correlation and hierarchical clustering*
309 To explore the relationships among the fruit shape descriptors, Pearson's correlation
310 coefficients were calculated using data of the ILs and AN-S-26 in both environments
311 (Supplementary data S1) and a hierarchical clustering heatmap analysis (Figure 3) was
312 performed. Both types of analyses provided congruent results, with the hierarchical clustering
313 analysis grouping traits into nine main clusters of correlated traits.
314 The cluster I comprised all the Basic Measurement descriptors and Eccentricity, among which
315 moderate to strong correlations were found (r = 0.59 to 1.00, $p < 0.001$) (Supplementary data
316 S1). Two sub-clusters could be distinguished within the cluster II. In the first sub-cluster, all
317 the Fruit shape Index descriptors, F_Shape_I, Circular and Ellipsoid resulted strongly
318 correlated (r = 0.71 to 1.00, $p < 0.001$) (Supplementary data S1). D_Blockiness, Obovoid,
319 Width_WP and Asob grouped together in the second sub-cluster, displaying moderate to strong
320 correlations (r = 0.59 to 0.95, $p < 0.001$). The cluster V comprised Triangle, PA_Macro, Ovoid
321 and Asov among which correlations varied from moderate to strong, with r values ranging from

0.37 ($p < 0.05$) to 0.98 ($p < 0.001$) (Supplementary data S1). Three descriptors were grouped in each of the clusters VI (P_Blockiness, Rectangular and Ec_Area) and VIII (DA_Micro, P_Eccentrcity and D_Eccentricity). In the cluster VI the correlations ranged from moderate to strong ($r = 0.61$ to 0.84, $p < 0.001$) (Table S1). In the cluster VIII, P_Eccentricity exhibited slight or moderate correlation with D_Eccentricity ($r = 0.42$, $p < 0.05$) and DA_Micro ($r = 0.51$, $p < 0.01$), respectively, while no correlation between D_Eccentricity and DA_Micro was found (Table S1). Asv, PA_Micro, SH_Height and DA_Macro showed no significant correlations with any other descriptors and were placed individually in four separated clusters (III, IV, VII and IX, respectively) (Supplementary data S1).

Hierarchical clustering grouped ILs and parent AN-S-26 in two main branches (Figure 3). The first branch comprised 4 clusters (A, B, C and D). Although clusters A and B consisted mainly of ILs grown in the open field, three of them corresponding to the screenhouse conditions (SMI_3.6_SH, SMI_5.1_SH and SMI_10.1_SH). The values for descriptors of the cluster I were generally high. In addition, cluster A showed high values for descriptors of cluster II. Cluster C grouped the recipient parent from both open field and screenhouse (AN-S-26_OF and AN-S-26_SH), showing high values for descriptors of the clusters II, VI and VII. Cluster D consisted mainly of ILs grown in the screenhouse except for one IL grown in the open field (SMI_8.1_OF), whose corresponding IL in screenhouse (SMI_8.1_SH) was also grouped in the same subcluster. In cluster D, values were especially high for SMI_3.5_SH and SMI_4.3_SH for the descriptors Ovoid and Asov of cluster V, while all the other descriptors were variable within the same cluster. The second branch comprised two clusters (E and F). Clusters E and F consisted only of ILs grown in screenhouse, except for one IL in cluster E (SMI_2.4_OF) that has its correspondent in cluster F. Clusters E and F exhibited low values for descriptors in clusters I and II, especially for the ILs SMI_2.4_SH, SMI_7.5_SH and

SMI_12.6_SH. In addition, cluster E exhibited low values even for descriptors in cluster VI, while cluster F showed high values for descriptors of most of the remaining clusters.

3.4. QTL detection

A total of 41 stable QTLs were found for 13 morphometric traits assessed with Tomato Analyzer in the IL set (Table 4 and Figure 4), with at least one QTL identified for each IL. Four stable QTLs were detected for Basic Measurement descriptors. Two of these QTLs (*wmh3* and *mw3*) were located on chromosome 3 (SMI_3.6), and the two others (*wmh10* and *mw10*) on chromosome 10 (SMI_10.1). The QTLs *wmh3* and *wmh10* accounted for an increase of Width_MH of 32.09% in OF and of 25.78% in SH, and of 48.96% in OF and of 26.25% in SH, respectively. In the same way, QTLs *mw3* and *mw10* displayed considerable effects for Max_Width, with an increase of 31.64% in OF and 25.52% in SH, and 48.6% in OF and 23.85% in SH, respectively. For Fruit Shape Index descriptors, 12 stable QTLs were detected on chromosomes 2, 3, 4 and 7. For each of the three descriptors (F_Shape_E_I, F_Shape_E_II and C_F_Shape) 4 QTLs spread over eight ILs (SMI_2.4, SMI_3.1, SMI_3.5, SMI_4.1, SMI_4.3, SMI_7.1, SMI_7.2 and SMI_7.5) were identified. These QTLs induced a considerable decrease over the recipient parent, ranging from -6.66% (*fseII3*) to -19.12% (*cfs7*) in OF, and from -10.71% (*fseI3*) to -47.57% (*fseII7*) in SH. For Blockiness descriptors, 4 stable QTLs were found to be distributed on chromosomes 1, 4, 8 and 12. Two QTLs (*pfb1*and *pfb12*) accounted for a decrease of P_Blockiness ranging from -11.45% to -15.45% in OF and from -18.82% to -22.07% in SH. Two QTLs (*dfb4* and *dfb8*) were involved in D_Blockiness variation, resulting in a D_Blockiness reduction of 9.37% in OF and 13.53% in SH, and of 16.31% in OF and 17.13% in SH, respectively. For Homogeneity descriptors, 10 stable QTLs were identified on chromosomes 1, 2, 3, 4, 5, 7, 10 and 12. The QTLs *eli4* and *eli7*, the first located in SMI_4.1 and SMI_4.3 and the latter in SMI_7.1, SMI_7.2 and SMI_7.5, accounted

for an Ellipsoid decrease ranging from -22.51% to -33.82% in OF, and from -22.01% to -39.17% in SH. The QTLs *cir2* (SMI_2.4), *cir3* (SMI_3.1 and SMI_3.5), *cir4* (SMI_4.1 and SMI_4.3) and *cir7* (SMI_7.1, SMI_7.2 and SMI_7.5) detected, exhibited large decrease effects on Circular ranging from -14.08% to -41.40% in OF and from -21.66% to -68.53% in SH. A considerable decrease over AN-S-26 parent was found for the QTLs *rec1* (SMI_1.1 and SMI_1.3), *rec5* (SMI_5.1), *rec10* (SMI_10.1) and *rec12* (SMI_12.6) that decreased the Rectangular descriptor values from -6.3% to -10.16% in OF and from -6.55% to -9.41% in SH. For Asymmetry descriptors, one QTL was identified on chromosome 8 (*obv8*). The effect of *obv8* resulted in a change of -35.75% in OF and -44.44% in SH of Obovoid, with a negative allelic effect between -0.04 and -0.05. For Internal Eccentricity descriptors, 10 stable QTLs were found spread in all chromosomes except for chromosomes 5, 6 and 11. The QTLs *fsi2* (SMI_2.4), *fsi3* (SMI_3.1 and SMI_3.5), *sfi4* (SMI_4.1 and SMI_4.3) and *fsi7* (SMI_7.1, SMI_7.2 and SMI_7.5) had a considerable decrease effect on F_Shape_I (from -7.73% to -19.86% in OF and from -10.54% to -46.44% in SH). Similarly, the QTLs *eca1* (SMI_1.1 and SMI_1.3), *eca4* (SMI_4.1 and SMI_4.3), *eca8* (SMI_8.1), *eca9* (SMI_9.1), *eca10* (SMI_10.1) and *eca12* (SMI_12.6) accounted for a decrease of Ec_Area ranging from -4.16% to -5.96% in OF and from -8.11% to -10.08% in SH.

QTLs controlling correlated descriptors co-localized in the same genomic region. In fact, the QTLs detected for Width_Mh and Max_Width co-localized in SMI_3.6 and SMI_10.1. In the same way, all the QTLs detected for F_Shape_E_I, F_Shape_E_II, F_C_Shape, Circular and F_Shape_I co-localized over eight ILs (SMI_2.4, SMI_3.1, SMI_3.5, SMI_4.1, SMI_4.3, SMI_7.1, SMI_7.2 and SMI_7.5).

3.5. Analysis of genetic variants in fruit shape related genes

A total of 118 homozygous allelic variants were identified in 43 out of 74 genes belonging to three selected gene families that control fruit shape in tomato (*SUN*, *OVATE* and *YABBY*). To test if a variant has an impact on the biological protein function, the effects of amino acid substitutions and indels were predicted using SIFT and PROVEAN software. A total of 36 variants with predicted high impact effects on protein function were found in 19 eggplant genes, of which 11 of them were located within the introgressed fragments of the ILs (Table 5). SIFT and PROVEAN classified as deleterious, respectively, 27 and 9 variants, with only one variant (L535W) considered deleterious by both software. All the remaining variants were classified as neutral, according to the prediction of both software (Supplementary data S2). SIFT predictions were not available for 4 substitutions (T123_A124insA, del354R, Q119dup and S171del), mainly because the amino acid change involved more than one nucleotide change within a codon.

4. Discussion

Fruit shape is a relevant morphological trait for eggplant breeding, and, like fruit size and color, is quantitatively inherited (Page et al., 2019). Despite its importance, compared to tomato, little information is available about the genetic basis of fruit shape in eggplant. QTLs and genes controlling traits associated to eggplant fruit shape have been previously detected by linkage mapping approach in interspecific and intraspecific F2 populations (Doganlar et al., 2002; Frary et al. 2014; Portis et al., 2014; Wei et al., 2020) and through genome-wide association studies (Portis et al., 2015). The present study is the first combining the use of an experimental introgression line population and a phenomics tool to enhance the precision in the detection of genomic regions controlling this quantitative trait.

As expected, many differences in fruit shape were found between the two parents, the cultivated *S. melongena* AN-S-26 and the wild relative *S. incanum* MM557, confirming that

diversification from small rounded to more elongated fruit occurred during eggplant domestication process (Wang et al., 2008). Although the hybrid set fruits only in the open field, it displayed negative heterosis for most fruit shape descriptors, so that they are skewed towards that of the wild parent. In this regard, Kaushik et al. (2016) observed that, in the case of crosses involving cultivated eggplants and wild species, generally, the hybrid fruit is phenotypically closer to its wild parent than to the cultivated one, probably due to the overall dominance of wild traits over the domesticated ones (Lester, 1989; Page et al., 2019). The negative heterotic values of the interspecific hybrid over the mid-parent for fruit shape traits are the opposite of the positive heterotic values observed for vigour-related traits in Mangino et al. (2020).

Significant differences found in fruit shape between ILs and the recipient parent suggested the existence of a relevant effect of the introgressions on this trait, even in presence of small wild donor fragments. This is in contrast with previously reported for morphological traits, for most of which the ILs showed minimal phenotypic differences compared to the recipient parent, even in the presence of large *S. incanum* introgressions (Mangino et al., 2020). This discrepancy can be explained due to the quantitative nature of both vigour-related traits of Mangino et al. (2020) and shape-related traits of this study. However, while for fruit shape, major genes have been described that affect substantially the phenotype, like *SUN*, *OVATE* or *FAS* in tomato (Liu et al., 2002; Xiao et al., 2008; Cong et al., 2008), no major genes have been reported so far that impact dramatically the plant vigour or morphology traits like those assessed in Mangino et al. (2020). Thus, it is likely that introgressions, even small, that carry some major genes, or with medium effects, on fruit shape can have a significative impact on fruit phenotype and exhibit significant differences with the recipient parent. Similarly, the same introgressions can carry genes that are involved in vigour or morphology traits, but their effects are too low to be considered as significant. Analysis of variance showed wide variations among fruit shape morphometric traits for the genotype factor contribution, environment, or G × E

interaction effects. Although the contribution of the environment and the G × E interaction was significant for almost all descriptors, their effects on fruit shape were relatively low. In fact, the contribution of genotype factor, in general, was the largest for many descriptors, indicating that the variation observed in fruit shape is mainly genetically regulated, as previously reported in tomato (El-Gabri et al., 2014; Monforte et al., 2014; Figàs et al., 2018). However, the fact that the contribution of the residual effect was the largest for many descriptors, might indicate that the influence of the environment was greater than genetic variability between the two parents for these specific traits. This is probably caused because for these traits there is little genetic variation among the ILs for these traits. The use of larger sample sizes might help to discern if some genetic variation exists among the ILs.

As found in previous studies in eggplant (Hurtado et al., 2013), tomato (Figas et al., 2015; Mohan et al., 2016) and pepper (Tripodi and Greco, 2018; Colonna et al., 2019), many Tomato Analyzer descriptors are interrelated, since they measure very similar shape characters. Here, nine clusters of highly correlated descriptors were observed, suggesting that, although Tomato Analyzer software can provide a good characterization of eggplant fruit shape (Prohens et al., 2012; Hurtado et al., 2013; Plazas et al., 2014; Kaushik et al., 2016, 2018), with fewer traits assessed we could obtain similar comprehensive information on this trait in eggplant.

In total, we identified 41 stable QTLs related to fruit shape, increasing the number of known QTLs in eggplant, particularly for fruit shape. In agreement with previous studies based on intraspecific population between eggplant lines ‘305E40’ and ‘67/3’ (Portis et al., 2014) and GWAS analysis (Portis et al., 2015), we detected four QTLs controlling fruit width, among which two (*wmh3.6* and *mw3.6*) were on chromosome 3 (SMI_3.6) and the two other (*wmh10.1* and *mw10.1*) on chromosome 10 (SMI_10.1). We found that *wmh3.6*/*wmh10.1* and *mw3.6*/*mw10.1* increased Width_MH between 26.3% and 49.0% and Max_Width between 23.9 and 48.7%, respectively, suggesting that *S. incanum* harbours QTLs which would make

the fruit wider. QTLs controlling fruit shape index in eggplant have been identified spread over many chromosomes (Doganlar et al., 2002; Frary et al., 2014; Portis et al., 2014; Portis et al., 2015; Wei et al., 2020). Using an F2 between *S. melongena* 'MM738' and *S. linneanum* 'MM195', Doganlar et al. (2002) identified two fruit-shape index related QTLs on chromosome 2 and 7 which explained between 34% to 36% of the variation for this trait. Portis et al. (2014) detected five major QTLs affecting fruit shape index on chromosomes 1, 3, 7, 11 and 12, and, subsequently, additional QTLs were detected on chromosome 5 and 10 (Portis et al., 2015). Moreover, a more recent study used an F2 population between *S. melongena* '1836' and *S. linneanum* '1809' reported four fruit shape index QTLs on chromosome 1 and 3 (Wei et al., 2020). In the present study, for each of the three Fruit shape index descriptors (F_Shape_E_I, F_Shape_E_II and C_F_Shape) we detected four stable QTLs spread over chromosomes 2, 3, 4 and 7, confirming the QTLs locations of previous studies. Moreover, probably thanks to the higher precision of the phenomic analysis made with Tomato Analyser, we could also confirm a site-specific and minor fruit shape index QTL identified on chromosome 4 by Portis et al. (2014), suggesting the importance of high-resolution morphometric tools and advanced introgressed materials in the detection of minor QTLs for the explanation of the phenotypic variation.

In addition, we have reported novel QTLs associated with Tomato Analyzer descriptors (Blockiness, Homogeneity, Asymmetry and Internal Eccentricity) that have not been assessed before in eggplant. Regarding D_Blockiness and P_Blockiness, we detected four QTLs in our lines being two of them syntenic to tomato (*pfb1* and *dfb8*) (Brewer et al., 2007; Gonzalo and van der Knaap, 2008). As well, we described novel QTLs on chromosomes 2, 3, 4 and 7 for F_Shape_I, which describes the shape of the internal ellipse drawn around the seed area, and on chromosomes 1, 4, 8, 9, 11 and 12 for Eccentricity area index (Ec_area), which explains the ratio of the ellipse area over total fruit area; some of them are syntenic to those identified in

tomato on chromosomes 2 and 8 (Gonzalo et al., 2009). We found that QTLs affecting ellipsoid or circular fruit shape were located on chromosomes 2 (*cir2*), 3 (*cir3*), 4 (*eli4* and *cir4*) and 7 (*eli7* and *cir7*), while rectangular fruit shape resulted affected by QTLs located on chromosomes 1 (*rec1*), 5 (*rec5*), 10 (*rec10*) and 12 (*rec12*). In tomato, long and oxheart fruit shape are often associated with mutations in *SUN* gene, mapped on chromosome 7, while obovoid, rectangular, ellipsoid, heart and pear fruit shape are often associated with mutations in the *OVATE* gene, mapped on chromosome 2 (Rodríguez et al. 2011). Our results suggest that rectangular fruit shape and ellipsoid/circular fruit shape are controlled by QTLs mapped to different chromosomes in eggplant. Moreover, of the six QTLs controlling ellipsoid and a circular shape in eggplant, one (*cir2*) and two (*eli7* and *cir7*) are syntenic to those of tomato on chromosome 2 and 7, respectively. We detected a QTL influencing obovoid fruit shape located on chromosome 8 (*obv8*). Similarly, a major QTL (*fs8.1*) controlling fruit shape in tomato by promoting the growth along the proximal-distal axis has been detected on chromosome 8 (Grandillo et al., 1996; Ku et al., 2000). Synteny between tomato and eggplant for the genomic region harboring *fs8.1* have been previously described by Portis et al. (2015). These evidences indicate the conservation of this QTL among some *Solanum* crops bearing fruits and suggest that in eggplant it could be involved in the regulation of obovoid fruit shape.

In general, we observed that QTLs detected for significantly correlated traits ($r > 0.9$) clustered within the same genomic regions. This might indicate that, what appear to be QTL clusters, probably, could be the result of a single pleiotropic locus, or, that different traits measured with Tomato Analyzer are assessing the same underlying character.

In the genomic regions where stable QTLs were detected, we assessed the presence of mutations in the genes of *SUN*, *OVATE* and *FAS* families from tomato that could be associated with the fruit shape variations in eggplant. Deleterious mutations (i.e., high-impact mutations) have been identified mainly in genes belonging to the *SUN* and *FAS* family, while in *OFP*

family, deleterious mutations have been identified for genes mapped outside the QTL regions. In the small QTL regions of the non-overlapping ILs SMI_2.4 and SMI_3.6, we identified deleterious mutations for the tomato syntenic genes *SlSUN7* and *SlSUN11*, which could be proposed as candidate genes involved in the control of fruit shape in eggplant. Although most candidate genes have been identified in QTL regions covering a broad segment of a chromosome, we found some congruences with previous studies. In fact, according to Huang et al. (2013) which proposed *SlSUN22* as the gene underlying the *fs8.1* locus in tomato, in this study *SlSUN22* mapped in the QTL region of chromosome 8 (SMI_8.1) and showed two deleterious mutations (V12I and I297V). These evidences suggest that, although other unknown genes located on the same genomic regions may be involved in the regulation of fruit shape, candidate genes that we have identified could have a great impact on the determination of fruit shape in eggplant.

5. Conclusions

In the present study, we have demonstrated the utility of combining the use of a powerful phenomics tool (Tomato Analyzer) with an experimental population (ILs) for a more precise identification of genomic regions controlling fruit shape in eggplant. This has allowed the detection of many phenotypic variations for fruit shape traits between ILs and recipient parent (*S. melongena*), even in the presence of small introgression from *S. incanum* parent. New stable QTLs for fruit shape traits first identified here in eggplant, as well as QTLs syntenic to those previously reported in tomato and eggplant populations, have been detected. In addition, in genomic regions underlying QTLs, we identified potential candidate genes syntenic to tomato ones belonging to the *SUN* and *YABBY* families that could have a significant effect on the fruit shape variations in eggplant. These findings are of great interest for eggplant breeding and make a relevant contribution to elucidate the genetic basis of fruit shape in this crop.

Supplementary information

Supplementary data S1. Pearson's correlation coefficients among the fruit shape descriptors using data of the ILs and AN-S-26 in both environments.

Supplementary data S2. Effect prediction on protein functionality using SIFT (Sorting Intolerant From Tolerant) (Ng and Henikoff, 2001) and PROVEAN (PROtein Variation Effect Analyzer) (Choi et al., 2012) software for the homozygous variants between the two parents of the IL population in eggplant genes identified as putative orthologous of tomato genes controlling fruit shape belonging to the SUN, OVATE and YABBY gene families described in Huang et al. (2013).

Funding

This work was undertaken as part of the initiative "Adapting Agriculture to Climate Change: Collecting, Protecting and Preparing Crop Wild Relatives", which is supported by the Government of Norway. The project is managed by the Global Crop Diversity Trust with the Millennium Seed Bank of the Royal Botanic Gardens, Kew and implemented in partnership with national and international gene banks and plant breeding institutes around the world. For further information see the project website: http://www.cwrdiversity.org/. Funding was also received from Spanish Ministerio de Economía, Industria y Competitividad and Fondo Europeo de Desarrollo Regional (grant AGL2015-64755-R from MINECO/FEDER), Ministerio de Ciencia, Innovación y Universidades, Agencia Estatal de Investigación and Fondo Europeo de Desarrollo Regional (grant RTI-2018-094592-B-100 from MCIU/AEI/FEDER, UE), and European Union's Horizon 2020 Research and Innovation Programme under grant agreement No. 677379 (G2P-SOL project: Linking genetic resources,

genomes and phenotypes of Solanaceous crops). Pietro Gramazio is grateful to Japan Society for the Promotion of Science for a post-doctoral grant (P19105, FY2019 JSPS Postdoctoral Fellowship for Research in Japan [Standard]).

Declaration of Competing Interest

The authors declare that they have no known competing financial interests or personal relationships that could have appeared to influence the work reported in this paper.

595 **References**

596 Alqudah, A.M., Sallam, A., Stephen Baenziger, P., Börner, A., 2020. GWAS: Fast-forwarding
597 gene identification and characterization in temperate Cereals: lessons from Barley – A
598 review. J. Adv. Res. 22, 119-135. https://doi.org/10.1016/j.jare.2019.10.013.

599 Anwar, R., Fatima, T., Mattoo, A., 2019. Tomatoes: A model crop of Solanaceous plants, in:
600 Oxford Research Encyclopedia of Environmental Science.
601 https://doi.org/10.1093/acrefore/9780199389414.013.223.

602 Balakrishnan, D., Surapaneni, M., Mesapogu, S., Neelamraju, S., 2019. Development and use
603 of chromosome segment substitution lines as a genetic resource for crop improvement.
604 Theor. Appl. Genet. 132, 1-25. https://doi.org/10.1007/s00122-018-3219-y.

605 Barrantes, W., López-Casado, G., García-Martínez, S., Alonso, A., Rubio, F., Ruiz, J.J.,
606 Fernández-Muñoz, R., Granell, A., Monforte, A.J., 2016. Exploring new alleles involved
607 in tomato fruit quality in an introgression line library of *Solanum pimpinellifolium*. Front.
608 Plant Sci. 7, 1172. https://doi.org/10.3389/fpls.2016.01172.

609 Bernacchi, D., Beck-Bunn, T., Eshed, Y., Lopez, J., Petiard, V., Uhlig, J., Zamir, D., Tanksley,
610 S., 1998. Advanced backcross QTL analysis in tomato. I. Identification of QTLs for traits
611 of agronomic importance from *Lycopersicon hirsutum*. Theor. Appl. Genet. 97, 381–397.
612 https://doi.org/10.1007/s001220050908.

613 Boopathi, N.M., 2020. Mapping population development. In: Boopathi, N.M. (Eds.), Genetic
614 mapping and marker assisted selection. Springer, Singapore, pp. 69-106.
615 https://doi.org/10.1007/978-981-15-2949-8_3

616 Brewer, M.T., Lang, L., Fujimura, K., Dujmovic, N., Gray, S., van der Knaap, E., 2006.
617 Development of a controlled vocabulary and software application to analyze fruit shape
618 variation in tomato and other plant species. Plant Physiol. 141, 15-25.
619 https://doi.org/10.1104/pp.106.077867.

Brewer, M.T., Moyseenko, J.B., Monforte, A.J., van der Knaap, E., 2007. Morphological variation in tomato: a comprehensive study of quantitative trait loci controlling fruit shape and development. J. Exp. Bot. 58, 1339-1349. https://doi.org/10.1093/jxb/erl301.

Can, H., Kal, U., Ozyigit, I.I., Paksoy, M., Turkmen, O., 2019. Construction, characteristics and high throughput molecular screening methodologies in some special breeding populations: a horticultural perspective. J. Genet. 98, 86. https://doi.org/10.1007/s12041-019-1129-7.

Celik, I., Gurbuz, N., Uncu, A.T., Frary, A., Doganlar, S., 2017. Genome-wide SNP discovery and QTL mapping for fruit quality traits in inbred backcross lines (IBLs) of *solanum pimpinellifolium* using genotyping by sequencing. BMC Genomics. 18, 1. https://doi.org/10.1186/s12864-016-3406-7.

Chakrabarti, M., Zhang, N., Sauvage, C., Muños, S., Blanca, J., Cañizares, J., Diez, M.J., Schneider, R., Mazourek, M., McClead, J., Causse, M., van der Knaap, E., 2013. A cytochrome P450 regulates a domestication trait in cultivated tomato. Proc. Natl. Acad. Sci. U. S. A. 110, 17125-17130. https://doi.org/10.1073/pnas.1307313110.

Choi, Y., Sims, G.E., Murphy, S., Miller, J.R., Chan, A.P., 2012. Predicting the functional effect of amino acid substitutions and indels. PLoS One. 7, e46688. https://doi.org/10.1371/journal.pone.0046688.

Cingolani, P., Platts, A., Wang, L.L., Coon, M., Nguyen, T., Wang, L., Land, S.J., Lu, X., Ruden, D.M., 2012. A program for annotating and predicting the effects of single nucleotide polymorphisms, SnpEff. Fly. 6, 80-92. https://doi.org/10.4161/fly.19695.

Colonna, V., D'Agostino, N., Garrison, E., Albrechtsen, A., Meisner, J., Facchiano, A., Cardi, T., Tripodi, P., 2019. Genomic diversity and novel genome-wide association with fruit morphology in *Capsicum*, from 746k polymorphic sites. Sci. Rep. 9, 10067. https://doi.org/10.1038/s41598-019-46136-5.

Cong, B., Barrero, L.S., Tanksley, S.D., 2008. Regulatory change in YABBY-like transcription factor led to evolution of extreme fruit size during tomato domestication. Nat. Genet. 40, 800–804. https://doi.org/10.1038/ng.144.

Costa, C., Antonucci, F., Pallottino, F., Aguzzi, J., Sun, D.W., Menesatti, P., 2011. Shape analysis of agricultural products: a review of recent research advances and potential application to computer vision. Food Bioprocess Technol. 4, 673–692. https://doi.org/10.1007/s11947-011-0556-0.

Di Giacomo, M., Luciani, M.D., Cambiaso, V., Zorzoli, R., Rodríguez, G.R., Pereira da Costa, J.H., 2020. Tomato near isogenic lines to unravel the genetic diversity of *S. pimpinellifolium* LA0722 for fruit quality and shelf life breeding. Euphytica. 216, 126. https://doi.org/10.1007/s10681-020-02649-z.

Díaz, A., Martín-Hernández, A.M., Dolcet-Sanjuan, R., Garcés-Claver, A., Álvarez, J.M., Garcia-Mas, J., Picó, B., Monforte, A.J., 2017. Quantitative trait loci analysis of melon (*Cucumis melo* L.) domestication-related traits. Theor. Appl. Genet. 130, 1837–1856. https://doi.org/10.1007/s00122-017-2928-y.

Doganlar, S., Frary, A., Daunay, M.C., Lester, R.N., Tanksley, S.D., 2002. Conservation of gene function in the Solanaceae as revealed by comparative mapping of domestication traits in eggplant. Genetics. 161, 1713-1726.

Daunay MC., 2008. Eggplant. In: Prohens J., Nuez F. (Eds.), Vegetables II. Handbook of plant breeding, vol 2. Springer, New York, pp. 163-220. https://doi.org/10.1007/978-0-387-74110-9_5.

El-Gabry, M.A.H., Solieman, T.I.H., Abido, A.I.A., 2014. Combining ability and heritability of some tomato (*Solanum lycopersicum* L.) cultivars. Sci. Hortic. 167, 153-157. https://doi.org/10.1016/j.scienta.2014.01.010.

669 Eshed, Y., Zamir, D., 1995. An introgression line population of *Lycopersicon pennellii* in the
670 cultivated tomato enables the identification and fine mapping of yield-associated QTL.
671 Genetics 141, 1147–1162.
672 Fasahat, P., 2016. Principles and utilization of combining ability in plant breeding. Biometrics
673 Biostat. Int. J. 4, 1-22. https://doi.org/10.15406/bbij.2016.04.00085.
674 Figàs, M.R., Prohens, J., Raigón, M.D., Fernández-de-Córdova, P., Fita, A., Soler, S., 2015.
675 Characterization of a collection of local varieties of tomato (*Solanum lycopersicum* L.)
676 using conventional descriptors and the high-throughput phenomics tool Tomato Analyzer.
677 Genet. Resour. Crop Evol. 62, 189–204. https://doi.org/10.1007/s10722-014-0142-1.
678 Figàs, M.R., Prohens, J., Casanova, C., Fernández-de-Córdova, P., Soler, S., 2018. Variation
679 of morphological descriptors for the evaluation of tomato germplasm and their stability
680 across different growing conditions. Sci. Hortic. 238, 107-115.
681 https://doi.org/10.1016/j.scienta.2018.04.039.
682 Frary, A., Fulton, T.M., Zamir, D., Tanksley, S.D., 2004. Advanced backcross QTL analysis
683 of a *Lycopersicon esculentum* x *L. pennellii* cross and identification of possible orthologs
684 in the Solanaceae. Theor. Appl. Genet. 108, 485–496. https://doi.org/10.1007/s00122-
685 003-1422-x.
686 Frary, Amy, Frary, Anne, Daunay, M.C., Huvenaars, K., Mank, R., Doğanlar, S., 2014. QTL
687 hotspots in eggplant (*Solanum melongena*) detected with a high resolution map and CIM
688 analysis. Euphytica. 197, 211–228. https://doi.org/10.1007/s10681-013-1060-6.
689 Gonzalo, M.J., van der Knaap, E., 2008. A comparative analysis into the genetic bases of
690 morphology in tomato varieties exhibiting elongated fruit shape. Theor. Appl. Genet. 116,
691 647–656. https://doi.org/10.1007/s00122-007-0698-7.
692 Gonzalo, M.J., Brewer, M.T., Anderson, C., Sullivan, D., Gray, S., van der Knaap, E., 2009.
693 Tomato fruit shape analysis using morphometric and morphology attributes implemented

694 in tomato analyzer software program. J. Am. Soc. Hortic. Sci. 134, 77-87.
695 https://doi.org/10.21273/jashs.134.1.77.
696 Gramazio, P., Prohens, J., Plazas, M., Mangino, G., Herraiz, F.J., Vilanova, S., 2017.
697 Development and genetic characterization of advanced backcross materials and an
698 introgression line population of *Solanum incanum* in a *S. melongena* background. Front.
699 Plant Sci. 8, 1477. https://doi.org/10.3389/fpls.2017.01477.
700 Gramazio, P., Yan, H., Hasing, T., Vilanova, S., Prohens, J., Bombarely, A., 2019. Whole-
701 genome resequencing of seven eggplant (*Solanum melongena*) and one wild relative (*S.*
702 *incanum*) accessions provides new insights and breeding tools for eggplant enhancement.
703 Front. Plant Sci. 10, 1220. https://doi.org/10.3389/fpls.2019.01220.
704 Grandillo, S., Ku, H.M., Tanksley, S.D., 1996. Characterization of *fs8.1*, a major QTL
705 influencing fruit shape in tomato. Mol. Breed. 2, 251–260.
706 https://doi.org/10.1007/BF00564202.
707 Gur, A., Zamir, D., 2015. Mendelizing all components of a pyramid of three yield QTL in
708 tomato. Front. Plant Sci. 6, 1096. https://doi.org/10.3389/fpls.2015.01096.
709 Haggard, J.E., Johnson, E.B., St. Clair, D.A., 2013. Linkage relationships among multiple QTL
710 for horticultural traits and late blight (*P. infestans*) resistance on chromosome 5
711 introgressed from wild tomato *Solanum habrochaites*. G3 Genes, Genomes, Genet. 3,
712 2131-2146. https://doi.org/10.1534/g3.113.007195.
713 Huang, Z., Van Houten, J., Gonzalez, G., Xiao, H., van der Knaap, E., 2013. Genome-wide
714 identification, phylogeny and expression analysis of *SUN*, *OFP* and *YABBY* gene family
715 in tomato. Mol. Genet. Genomics. 288, 111–129. https://doi.org/10.1007/s00438-013-
716 0733-0.
717 Hurtado, M., Vilanova, S., Plazas, M., Gramazio, P., Fonseka, H.H., Fonseka, R., Prohens, J.,
718 2012. Diversity and relationships of eggplants from three geographically distant

719 secondary centers of diversity. PLoS One. 7, e41748.
720 https://doi.org/10.1371/journal.pone.0041748.
721 Hurtado, M., Vilanova, S., Plazas, M., Gramazio, P., Herraiz, F.J., Andújar, I., Prohens, J.,
722 2013. Phenomics of fruit shape in eggplant (*Solanum melongena* L.) using Tomato
723 Analyzer software. Sci. Hortic. 164, 625-632.
724 https://doi.org/10.1016/j.scienta.2013.10.028.
725 IPGRI (1996) Descriptors for tomato (*Lycopersicon* spp.). International Plant Genetic
726 Resources Institute, Rome.
727 Kaushik, P., Prohens, J., Vilanova, S., Gramazio, P., Plazas, M., 2016. Phenotyping of eggplant
728 wild relatives and interspecific hybrids with conventional and phenomics descriptors
729 provides insight for their potential utilization in breeding. Front. Plant Sci. 7, 677.
730 https://doi.org/10.3389/fpls.2016.00677.
731 Kaushik, P., Plazas, M., Prohens, J., Vilanova, S., Gramazio, P., 2018. Diallel genetic analysis
732 for multiple traits in eggplant and assessment of genetic distances for predicting hybrids
733 performance. PLoS One. 13, e0199943. https://doi.org/10.1371/journal.pone.0199943.
734 Kim, H., Kim, B.S., Shim, J.E., Hwang, S., Yang, S., Kim, E., Iyer-Pascuzzi, A.S., Lee, I.,
735 2017. TomatoNet: A genome-wide co-functional network for unveiling complex traits of
736 tomato, a model crop for fleshy fruits. Mol. Plant. 10, 652-655.
737 https://doi.org/10.1016/j.molp.2016.11.010.
738 Kimura, S., Sinha, N., (2008). Tomato (*Solanum lycopersicum*): a model fruit-bearing crop.
739 Cold Spring Harb. Protoc. 3, 1-9. https://doi:10.1101/pdb.emo105.
740 Klee, H.J., Resende, M.F.R., 2020. Plant domestication: reconstructing the route to modern
741 tomatoes. Curr. Biol. 8, 359-361. https://doi.org/10.1016/j.cub.2020.02.072.

Ku, H.M., Grandillo, S., Tanksley, S.D., 2000. *fs8.1*, a major QTL, sets the pattern of tomato carpel shape well before anthesis. Theor. Appl. Genet. 101, 873–878. https://doi.org/10.1007/s001220051555.

Lester R.N., 1989. Evolution under domestication involving disturbance of genic balance. Euphytica 44, 125– 132. https://doi.org/10.1007/BF00022606.

Lippman, Z., Tanksley, S.D., 2001. Dissecting the genetic pathway to extreme fruit size in tomato using a cross between the small-fruited wild species *Lycopersicon pimpinellifolium* and *L. esculentum* var. Giant Heirloom. Genetics. 158, 413-422.

Liu, J., Van Eck, J., Cong, B., Tanksley, S.D., 2002. A new class of regulatory genes underlying the cause of pear-shaped tomato fruit. Proc. Natl. Acad. Sci. U. S. A. 99, 13302-13306. https://doi.org/10.1073/pnas.162485999.

Mangino, G., Plazas, M., Vilanova, S., Prohens, J., Gramazio, P., 2020. Performance of a set of eggplant (*Solanum melongena*) lines with introgressions from its wild relative *S. incanum* under open field and screenhouse conditions and detection of QTLs. Agronomy. 10, 467. https://doi.org/10.3390/agronomy10040467.

Mata-Nicolás, E., Montero-Pau, J., Gimeno-Paez, E., Garcia-Carpintero, V., Ziarsolo, P., Menda, N., Mueller, L.A., Blanca, J., Cañizares, J., van der Knaap, E., Díez, M.J., 2020. Exploiting the diversity of tomato: the development of a phenotypically and genetically detailed germplasm collection. Hortic. Res. 7, 66. https://doi.org/10.1038/s41438-020-0291-7.

Metsalu, T., Vilo, J., 2015. ClustVis: A web tool for visualizing clustering of multivariate data using Principal Component Analysis and heatmap. Nucleic Acids Res. 43, 566-570. https://doi.org/10.1093/nar/gkv468.

Mohan, V., Gupta, S., Thomas, S., Mickey, H., Charakana, C., Chauhan, V.S., Sharma, K., Kumar, R., Tyagi, K., Sarma, S., Gupta, S.K., Kilambi, H.V., Nongmaithem, S., Kumari,

767 A., Gupta, P., Sreelakshmi, Y., Sharma, R., 2016. Tomato fruits show wide phenomic
768 diversity but fruit developmental genes show low genomic diversity. PLoS One. 11,
769 e0152907. https://doi.org/10.1371/journal.pone.0152907.
770 Monforte, A.J., Tanksley, S.D., 2000. Development of a set of near isogenic and backcross
771 recombinant inbred lines containing most of the *Lycopersicon hirsutum* genome in a *L.*
772 *esculentum* genetic background: A tool for gene mapping and gene discovery. Genome.
773 43, 5. https://doi.org/10.1139/g00-043.
774 Monforte, A.J., Friedman, E., Zamir, D., Tanksley, S.D., 2001. Comparison of a set of allelic
775 QTL-NILs for chromosome 4 of tomato: Deductions about natural variation and
776 implications for germplasm utilization. Theor. Appl. Genet. 102, 572–590.
777 https://doi.org/10.1007/s001220051684.
778 Monforte, A.J., Diaz, A., Caño-Delgado, A., van der Knaap, E., 2014. The genetic basis of fruit
779 morphology in horticultural crops: lessons from tomato and melon. J. Exp. Bot. 65, 4625–
780 4637. https://doi.org/10.1093/jxb/eru017.
781 Nadeem, M.A., Nawaz, M.A., Shahid, M.Q., Doğan, Y., Comertpay, G., Yıldız, M., Hatipoğlu,
782 R., Ahmad, F., Alsaleh, A., Labhane, N., Özkan, H., Chung, G., Baloch, F.S., 2018. DNA
783 molecular markers in plant breeding: current status and recent advancements in genomic
784 selection and genome editing. Biotechnol. Biotechnol. Equip. 32, 261-285.
785 https://doi.org/10.1080/13102818.2017.1400401.
786 Nankar, A.N., Tringovska, I., Grozeva, S., Todorova, V., Kostova, D., 2020. Application of
787 high-throughput phenotyping tool Tomato Analyzer to characterize Balkan *Capsicum*
788 fruit diversity. Sci. Hortic. 260, 108862. https://doi.org/10.1016/j.scienta.2019.108862.
789 Ng, P.C., Henikoff, S., 2001. Predicting deleterious amino acid substitutions. Genome Res. 11,
790 863-874. https://doi.org/10.1101/gr.176601.

791 Oren, E., Tzuri, G., Dafna, A., Meir, A., Kumar, R., Katzir, N., Elkind, Y., Freilich, S.,
792 Schaffer, A.A., Tadmor, Y., Burger, J., Gur, A., 2020. High-density NGS-based map
793 construction and genetic dissection of fruit shape and rind netting in *Cucumis melo*. Theor.
794 Appl. Genet. 133, 1927–1945. https://doi.org/10.1007/s00122-020-03567-3.
795 Page A.M.L., Daunay MC., Aubriot X., Chapman M.A., 2019. Domestication of eggplants: A
796 phenotypic and genomic insight. In: Chapman M. (Eds.), The Eggplant Genome.
797 Springer, Cham, pp. 193-212. https://doi.org/10.1007/978-3-319-99208-2_12.
798 Pan, Y., Wang, Y., McGregor, C., Liu, S., Luan, F., Gao, M., Weng, Y., 2020. Genetic
799 architecture of fruit size and shape variation in cucurbits: a comparative perspective.
800 Theor. Appl. Genet. 133, 1–21. https://doi.org/10.1007/s00122-019-03481-3.
801 Paran, I., van der Knaap, E., 2007. Genetic and molecular regulation of fruit and plant
802 domestication traits in tomato and pepper. J. Exp. Bot. 58, 3841–3852.
803 https://doi.org/10.1093/jxb/erm257.
804 Pereira-Dias, L., Fita, A., Vilanova, S., Sánchez-López, E., Rodríguez-Burruezo, A., 2020.
805 Phenomics of elite heirlooms of peppers (*Capsicum annuum* L.) from the Spanish centre
806 of diversity: Conventional and high-throughput digital tools towards varietal typification.
807 Sci. Hortic. 265, 109245. https://doi.org/10.1016/j.scienta.2020.109245.
808 Plazas, M., Andújar, I., Vilanova, S., Gramazio, P., Javier Herraiz, F., Prohens, J., 2014.
809 Conventional and phenomics characterization provides insight into the diversity and
810 relationships of hypervariable scarlet (*Solanum aethiopicum* L.) and gboma (*S.*
811 *macrocarpon* L.) eggplant complexes. Front. Plant Sci. 5, 318.
812 https://doi.org/10.3389/fpls.2014.00318.
813 Portis, E., Barchi, L., Toppino, L., Lanteri, S., Acciarri, N., Felicioni, N., Fusari, F., Barbierato,
814 V., Cericola, F., Valè, G., Rotino, G.L., 2014. QTL mapping in eggplant reveals clusters

of yield-related loci and orthology with the tomato genome. PLoS One. 9, e89499. https://doi.org/10.1371/journal.pone.0089499.

Portis, E., Cericola, F., Barchi, L., Toppino, L., Acciarri, N., Pulcini, L., Sala, T., Lanteri, S., Rotino, G.L., 2015. Association mapping for fruit, plant and leaf morphology traits in eggplant. PLoS One. 10, e0135200. https://doi.org/10.1371/journal.pone.0135200.

Prohens, J., Plazas, M., Raigón, M.D., Seguí-Simarro, J.M., Stommel, J.R., Vilanova, S., 2012. Characterization of interspecific hybrids and first backcross generations from crosses between two cultivated eggplants (*Solanum melongena* and *S. aethiopicum* Kumba group) and implications for eggplant breeding. Euphytica. 186, 517–538. https://doi.org/10.1007/s10681-012-0652-x.

Ranil, R.H.G., Niran, H.M.L., Plazas, M., Fonseka, R.M., Fonseka, H.H., Vilanova, S., Andújar, I., Gramazio, P., Fita, A., Prohens, J., 2015. Improving seed germination of the eggplant rootstock *Solanum torvum* by testing multiple factors using an orthogonal array design. Sci. Hortic. 193, 174-181. https://doi.org/10.1016/j.scienta.2015.07.030.

Rodríguez, G., Strecker, J., Brewer, M., Gonzalo, M.J., Anderson, C., Lang, L., Sullivan, D., Wagner, E., Strecker, B., Drushal, R., Dujmovic, N., Fujimuro, K., Jack, A., Njanji, I., Thomas, J., Gray, S., Knaap, E. van der, 2010a. Tomato Analyzer Version 3 User Manual. https://vanderknaaplab.uga.edu/files/Tomato_Analyzer_3.0_Manual.pdf.

Rodríguez, G.R., Moyseenko, J.B., Robbins, M.D., Morejón, N.H., Francis, D.M., van der Knaap, E., 2010b. Tomato analyzer: A useful software application to collect accurate and detailed morphological and colorimetric data from two-dimensional objects. J. Vis. Exp. e1856. https://doi.org/10.3791/1856.

Rodríguez, G.R., Muños, S., Anderson, C., Sim, S.C., Michel, A., Causse, M., McSpadden Gardener, B.B., Francis, D., van der Knaap, E., 2011. Distribution of *SUN*, *OVATE*, *LC*,

and *FAS* in the tomato germplasm and the relationship to fruit shape diversity. Plant Physiol. 156, 275-285. https://doi.org/10.1104/pp.110.167577.

Rodríguez, G.R., Kim, H.J., van der Knaap, E., 2013. Mapping of two suppressors of *OVATE* (*sov*) loci in tomato. Heredity 111, 256–264. https://doi.org/10.1038/hdy.2013.45.

Sacco, A., Di Matteo, A., Lombardi, N., Trotta, N., Punzo, B., Mari, A., Barone, A., 2013. Quantitative trait loci pyramiding for fruit quality traits in tomato. Mol. Breed. 31, 217–222. https://doi.org/10.1007/s11032-012-9763-2.

Salvi, S., Tuberosa, R., 2005. To clone or not to clone plant QTLs: present and future challenges. Trends Plant Sci. 10, 297-304. https://doi.org/10.1016/j.tplants.2005.04.008.

Scott, J.W., 2010. Phenotyping of tomato for SolCAP and onward into the void. HortScience. 45, 1314–1316. https://doi.org/10.21273/hortsci.45.9.1314.

Snouffer, A., Kraus, C., van der Knaap, E., 2020. The shape of things to come: ovate family proteins regulate plant organ shape. Curr. Opin. Plant Biol. 53, 98-105. https://doi.org/10.1016/j.pbi.2019.10.005.

Tanksley, S.D., 2004. The genetic, developmental, and molecular bases of fruit size and shape variation in tomato. Plant Cell. 16, 181-189. https://doi.org/10.1105/tpc.018119.

Tripodi, P., Greco, B., 2018. Large scale phenotyping provides insight into the diversity of vegetative and reproductive organs in a wide collection of wild and domesticated peppers (*Capsicum* spp.). Plants. 7, 103. https://doi.org/10.3390/plants7040103.

UPOV (2017) Test Guidelines. http://www.upov.int/en/publications/tg-rom/tg_index.

van der Knaap, E., Tanksley, S.D., 2003. The making of a bell pepper-shaped tomato fruit: identification of loci controlling fruit morphology in Yellow Stuffer tomato. Theor. Appl. Genet. 107, 139–147. https://doi.org/10.1007/s00122-003-1224-1.

van der Knaap, E., Østergaard, L., 2018. Shaping a fruit: Developmental pathways that impact growth patterns. Semin. Cell Dev. Biol. 79, 27-36. https://doi.org/10.1016/j.semcdb.2017.10.028.

Wang, JX., Gao TG., Knapp, S., 2008. Ancient Chinese literature reveals pathways of eggplant domestication. Annals of Botany. 102, 891–897. https://doi.org/10.1093/aob/mcn179.

Wei, Q., Wang, W., Hu, T., Hu, H., Wang, J., Bao, C., 2020. Construction of a SNP-based genetic map using SLAF-Seq and QTL analysis of morphological traits in eggplant. Front. Genet. 11, 178. https://doi.org/10.3389/fgene.2020.00178.

Wu, S., Zhang, B., Keyhaninejad, N., Rodríguez, G.R., Kim, H.J., Chakrabarti, M., Illa-Berenguer, E., Taitano, N.K., Gonzalo, M.J., Díaz, A., Pan, Y., Leisner, C.P., Halterman, D., Buell, C.R., Weng, Y., Jansky, S.H., van Eck, H., Willemsen, J., Monforte, A.J., Meulia, T., van der Knaap, E., 2018. A common genetic mechanism underlies morphological diversity in fruits and other plant organs. Nat. Commun. 9, 4734. https://doi.org/10.1038/s41467-018-07216-8.

Xiao, H., Jiang, N., Schaffner, E., Stockinger, E.J., van der Knaap, E., 2008. A retrotransposon-mediated gene duplication underlies morphological variation of tomato fruit. Science. 319, 1527-1530. https://doi.org/10.1126/science.1153040.

Yan, G., Liu, H., Wang, H., Lu, Z., Wang, Y., Mullan, D., Hamblin, J., Liu, C., 2017. Accelerated generation of selfed pure line plants for gene identification and crop breeding. Front. Plant Sci. 8, 1786. https://doi.org/10.3389/fpls.2017.01786.

Yates, H.E., Frary, A., Doganlar, S., Frampton, A., Eannetta, N.T., Uhlig, J., Tanksley, S.D., 2004. Comparative fine mapping of fruit quality QTLs on chromosome 4 introgressions derived from two wild tomato species. Euphytica. 135, 283–296. https://doi.org/10.1023/B:EUPH.0000013314.04488.87.

886 Yin X., Struik, P.C., 2016. Modelling QTL-trait-crop relationships: Past experiences and future
887 prospects. In: Yin X., Struik, P.C. (Eds.), Crop Systems Biology. Springer, Cham, pp.
888 193-218. https://doi.org/10.1007/978-3-319-20562-5_9.
889 Zamir, D., 2001. Improving plant breeding with exotic genetic libraries. Nat. Rev. Genet. 2,
890 983–989. https://doi.org/10.1038/35103590.

Tables

Table 1. List of the 32 traits with respective codes and descriptions used for morphometric analysis with Tomato Analyzer v 3.0 software (Rodríguez et al., 2010a) of the 16 ILs, their parents (*S. melongena* AN-S-26 and *S. incanum* MM557) and the interspecific hybrid between them assessed in this study. Further details on the descriptors are available at the Tomato Analyzer software webpage (https://vanderknaaplab.uga.edu/tomato_analyzer.html).

Trait (Unit)	Code	Description
Basic Measurements		
Perimeter (cm)	Perimeter	Perimeter length
Area (cm^2)	Area	Fruit area
Width Mid-Height (cm)	Width_MH	The width measured at $^1/_2$ of the fruit's height
Maximum Width (cm)	Max_Width	The maximum horizontal distance of the fruit
Height Mid-Width (cm)	Height_MW	The height measured at $^1/_2$ of the fruit's width
Maximum Height (cm)	Max_Height	The maximum vertical distance of the fruit
Curved Height (cm)	C_Height	The height measured along a curved line through the fruit
Fruit Shape Index		
Fruit Shape Index External I	F_Shape_E_I	The ratio of the maximum height to the maximum width
Fruit Shape Index External II	F_Shape_E_II	The ratio of height mid-width to width mid-height
Curved Fruit Shape Index	C_F_Shape	The ratio of curved height to the width of the fruit at mid-curved-height, as measured perpendicular to the curved height line
Blockiness		
Proximal Fruit Blockiness	P_Blockiness	The ratio of the width at the upper blockiness position to width mid-height
Distal Fruit Blockiness	D_Blockiness	The ratio of the width at the lower blockiness position to width mid-height
Fruit Shape Triangle	Triangle	The ratio of the width at the upper blockiness position to the width at the lower blockiness position
Homogeneity		
Ellipsoid	Ellipsoid	The ratio of the error resulting from a best-fit ellipse to the area of the fruit; smaller values indicate that the fruit is more ellipsoid
Circular	Circular	The ratio of the error resulting from a best-fit circle to the area of the fruit; smaller values indicate that the fruit is more circular

Rectangular	Rectangular	The ratio of the area of the rectangle bounding the fruit to the area of the rectangle bounded by the fruit
Proximal Fruit End Shape		
Shoulder Height	Sh_Height	The ratio of the average height of the shoulder points above the proximal endpoint to the maximum height
Proximal Angle Micro (°)	PA_Micro	Proximal fruit end shape angle at position 1% above the tip from the fruit
Proximal Angle Macro (°)	PA_Macro	Proximal fruit end shape angle at position 5% above the tip from the fruit
Distal Fruit End Shape		
Distal Angle Micro (°)	DA_Micro	Distal fruit end shape angle at position 1% above the tip from the fruit
Distal Angle Macro (°)	DA_Macro	Distal fruit end shape angle at position 5% above the tip from the fruit
Asymmetry		
Obovoid	Obovoid	If the area of the fruit is greater below mid-height than above it, a function of width and height
Ovoid	Ovoid	If the area of the fruit is greater above mid-height than below it, a function of width and height
V. Asymmetry	Asv	The average distance between a vertical line through the fruit at mid-width and the midpoint of the fruit's width at each height
H. Asymmetry. Ob	Asob	If the area of the fruit is greater below mid-height than above it, a function of width and height
H. Asymmetry. Ov	Asov	If the area of the fruit is greater above mid-height than below it, a function of width and height
Width Widest Pos	Width_WP	The ratio of the height at which the maximum width occurs to the maximum height
Internal Eccentricity		
Eccentricity	Eccentricity	The ratio of the height of the internal ellipse to the maximum height
Proximal Eccentricity	P_Eccentricity	The ratio of the height of the internal ellipse to the distance between the bottom of the ellipse and the top of the fruit
Distal Eccentricity	D_Eccentricity	The ratio of the height of the internal ellipse to the distance between the top of the ellipse and the bottom of the fruit
Fruit Shape Index Internal	F_Shape_I	The ratio of the internal ellipse's height to its width
Eccentricity Area Index	Ec_Area	The ratio of the area of the fruit outside the ellipse to the total area of the fruit

898

899

Table 2. Means with standard errors and range values for the recipient parent (*S. melongena* AN-S-26), the donor parent (*S. incanum* MM577) and the interspecific hybrid (F1) of the IL population and hybrid mid-parent heterosis (H_{MP}) in the open field and screenhouse conditions and significance of differences of comparisons of screenhouse vs. open field for AN-S-26, MM577 vs. AN-S-26 for open field, and difference from 0 for H_{MP}.

	AN-S-26				MM577		F1		
	Open field		Screenhouse		Open field		Open field		
Trait (Unit)	**Mean**	**Range**	**Mean[a, b]**	**Range**	**Mean[a, c]**	**Range**	**Mean**	**Range**	**H_{MP}[a]**
Basic Measurements									
Perimeter	18.59 ± 1.40	15.36-22.99	21.11 ± 1.01^{ns}	17.25-23.26	6.40 ± 0.35***	5.41-7.29	12.11 ± 0.44	10.85-13.30	-0.020^{ns}
Area	22.48 ± 3.41	14.73-33.70	28.11 ± 2.64^{ns}	18.52-34.45	2.96 ± 0.32***	2.10-3.73	10.24 ± 0.71	8.00-12.02	-0.140^{ns}
Width_MH	4.00 ± 0.34	3.11-5.08	4.20 ± 0.20^{ns}	3.60-4.77	1.84 ± 0.11***	1.53-2.07	3.19 ± 0.10	2.90-3.43	0.108^{ns}
Max_Width	4.10 ± 0.35	3.21-5.25	4.38 ± 0.21^{ns}	3.70-4.96	1.85 ± 0.11***	1.54-2.09	3.21 ± 0.09	2.92-3.45	0.094^{ns}
Height_MW	6.56 ± 0.42	5.69-7.78	7.61 ± 0.36^{ns}	6.27-8.36	2.00 ± 0.09***	1.75-2.26	3.93 ± 0.16	3.44-4.34	-0.072^{ns}
Max_Height	6.65 ± 0.43	5.73-7.90	7.72 ± 0.37^{ns}	6.33-8.41	2.02 ± 0.10***	1.76-2.32	3.96 ± 0.16	3.46-4.37	-0.078^{ns}
C_Height	6.71 ± 0.42	5.8-7.93	7.85 ± 0.34^{ns}	6.53-8.48	2.15 ± 0.09***	1.91-2.37	4.08 ± 0.16	3.62-4.48	-0.071^{ns}
Fruit Shape Index									
F_Shape_E_I	1.64 ± 0.05	1.5-1.79	1.77 ± 0.05^{ns}	1.65-1.89	1.10 ± 0.03***	1.02-1.17	1.23 ± 0.02	1.19-1.28	-0.099*
F_Shape_E_II	1.67 ± 0.06	1.52-1.85	1.82 ± 0.06^{ns}	1.66-1.97	1.10 ± 0.03***	1.02-1.18	1.23 ± 0.02	1.19-1.27	-0.104*
C_F_Shape	1.70 ± 0.06	1.56-1.87	1.87 ± 0.06^{ns}	1.72-2.03	1.18 ± 0.03***	1.10-1.28	1.28 ± 0.02	1.24-1.34	-0.112*

Blockiness									
P_Blockiness	0.61 ± 0.02	0.55-0.66	0.63 ± 0.01^{ns}	0.62-0.65	0.57 ± 0.01^{ns}	0.53-0.61	0.59 ± 0.01	0.55-0.61	0.012^{ns}
D_Blockiness	0.75 ± 0.02	0.70-0.81	0.77 ± 0.02^{ns}	0.71-0.81	0.60 ± 0.01***	0.57-0.63	0.66 ± 0.00	0.65-0.67	-0.029^{ns}
Triangle	0.81 ± 0.02	0.75-0.87	0.83 ± 0.02^{ns}	0.76-0.89	0.95 ± 0.03**	0.87-1.02	0.91 ± 0.02	0.83-0.95	0.033^{ns}
Homogeneity									
Ellipsoid	0.05 ± 0.00	0.04-0.05	0.06 ± 0.00*	0.05-0.06	0.02 ± 0.00***	0.01-0.03	0.02 ± 0.00	0.02-0.02	-0.290***
Circular	0.16 ± 0.01	0.14-0.18	0.19 ± 0.01*	0.16-0.21	0.04 ± 0.01***	0.02-0.06	0.07 ± 0.00	0.06-0.08	-0.292**
Rectangular	0.53 ± 0.01	0.51-0.55	0.52 ± 0.01^{ns}	0.50-0.54	0.48 ± 0.01***	0.47-0.50	0.51 ± 0.00	0.50-0.52	0.008^{ns}
Proximal Fruit End Shape									
Sh_Height	0.04 ± 0.01	0.00-0.06	0.02 ± 0.01^{ns}	0.00-0.04	0.00 ± 0.00*	0.00-0.01	0.01 ± 0.01	0.00-0.04	-0.375^{ns}
PA_Micro	121.7 ± 4.3	110.0-135.8	129. ± 11.8^{ns}	87.0-158.8	156.3 ± 4.9***	146.4-174.6	151.7 ± 2.8	141.3-157.9	0.093*
PA_Macro	111.2 ± 3.9	105.1-125.8	110.7 ± 2.7^{ns}	105.5121.0	135.9 ± 1.8***	130.0-141.1	134.1 ± 2.7	124.6-139.6	0.089^{ns}
Distal Fruit End Shape									
DA_Micro	133.2 ± 19.0	70.3-175.1	130.3 ± 14.3^{ns}	98.8-176.4	151.3 ± 10.2^{ns}	111.8-170.3	135.1 ± 15.2	108.0-179.0	-0.040^{ns}
DA_Macro	135.2 ± 5.4	123.8-154.9	122.9 ± 8.2^{ns}	91.1-136.4	141.9 ± 2.6^{ns}	134.8-148.2	145.5 ± 0.8	143.1-148.0	0.053^{ns}
Asymmetry									
Obovoid	0.22 ± 0.02	0.18-0.27	0.24 ± 0.02^{ns}	0.21-0.29	0.10 ± 0.01***	0.06-0.12	0.11 ± 0.01	0.08-0.14	-0.264**

Ovoid	0.00 ± 0.00	0.00-0.00	0.00 ± 0.00^{ns}	0.00-0.00	0.02 ± 0.02^{ns}	0.00-0.08	0.02 ± 0.02	0.00-0.09	0.489^{ns}
Asv	0.06 ± 0.01	0.04-0.08	0.12 ± 0.02*	0.06-0.17	0.02 ± 0.00**	0.02-0.03	0.03 ± 0.00	0.03-0.04	-0.111^{ns}
Asob	0.24 ± 0.04	0.17-0.38	0.32 ± 0.04^{ns}	0.22-0.42	0.02 ± 0.00***	0.02-0.02	0.06 ± 0.01	0.03-0.07	-0.573**
Asov	0.00 ± 0.00	0.00-0.00	0.00 ± 0.00^{ns}	0.00-0.00	0.01 ± 0.01^{ns}	0.00-0.03	0.00 ± 0.00	0.00-0.02	0.378^{ns}
Width_WP	0.59 ± 0.02	0.54-0.64	0.62 ± 0.02^{ns}	0.58-0.67	0.48 ± 0.01***	0.46-0.50	0.50 ± 0.01	0.49-0.52	-0.063*
Internal Eccentricity									
Eccentricity	0.79 ± 0.00	0.78-0.79	0.78 ± 0.01^{ns}	0.74-0.80	0.79 ± 0.00^{ns}	0.78-0.80	0.79 ± 0.00	0.79-0.79	0.004^{ns}
P_Eccentricity	0.89 ± 0.00	0.88-0.89	0.88 ± 0.01^{ns}	0.85-0.89	0.89 ± 0.00^{ns}	0.89-0.90	0.89 ± 0.00	0.89-0.89	-0.002*
D_Eccentricity	0.89 ± 0.00	0.88-0.89	0.89 ± 0.00^{ns}	0.88-0.89	0.88 ± 0.00^{ns}	0.87-0.89	0.89 ± 0.00	0.88-0.89	0.001^{ns}
F_Shape_I	1.66 ± 0.06	1.51-1.85	1.79 ± 0.05^{ns}	1.64-1.97	1.10 ± 0.03***	1.02-1.18	1.23 ± 0.02	1.18-1.27	-0.106*
Ec_Area	0.40 ± 0.01	0.39-0.41	0.41 ± 0.01^{ns}	0.39-0.44	0.37 ± 0.00**	0.36-0.38	0.38 ± 0.00	0.37-0.39	-0.011^{ns}

[a]***, **, *, ns indicate respectively, significant differences at p values <0.001, <0.01, and <0.05 or not significative ($p \geq 0.05$).

[b]Significances correspond to the comparison of screenhouse vs. open field conditions for AN-S-26.

[c]Significances correspond to the comparison of MM577 vs. AN-S-26 for open field conditions.

Table 3. Percentage and statistical significance of the sums of squares over the total for the genotype, environment, genotype × environment (G × E), block and residual effects calculated with a two-way ANOVA to evaluate the differences among ILs and the recurrent parent AN-S-26.

	Sums of squares				
Trait	**Genotype**	**Environment**	**G × E**	**Block**	**Residual**
Basic Measurements					
Perimeter	28.23***	18.75***	18.35***	5.78	28.89
Area	27.63***	18.00***	15.75***	6.48	32.14
Width_MH	33.93***	13.85***	10.90**	7.03	34.29
Max_Width	31.37***	15.75***	11.36**	7.41	34.11
Height_MW	31.52***	20.90***	19.69***	4.73	23.16
Max_Height	30.38***	20.70***	19.58***	5.03	24.31
C_Height	30.63***	20.03***	19.75***	4.89	24.7
Fruit Shape Index					
F_Shape_E_I	49.08***	9.65***	19.11***	1.12	21.04
F_Shape_E_II	47.45***	10.32***	19.79***	0.72	21.72
C_F_Shape	47.85***	8.20***	19.28***	0.6	24.07
Blockiness					
P_Blockiness	44.74***	4.24**	8.43^{ns}	2.21	40.38
D_Blockiness	43.72***	1.75**	17.31***	1.83	35.39
Triangle	44.06***	5.99***	6.23^{ns}	2.44	41.28
Homogeneity					
Ellipsoid	39.64***	2.31***	24.40***	0.88	32.77
Circular	48.94***	9.29***	20.28***	0.78	20.71

Rectangular	40.17***	2.49**	13.04**	2.55	41.75
Proximal Fruit End Shape					
Sh_Height	23.48***	1.25^{ns}	14.32*	3.02	57.93
PA_Micro	7.14^{ns}	0.95^{ns}	6.31^{ns}	4.45	81.15
PA_Macro	43.99***	13.28***	10.2**	1.75	30.78
Distal Fruit End Shape					
DA_Micro	16.64*	2.14*	16.70*	3.38	61.14
DA_Macro	13.48^{ns}	0.13^{ns}	12.02^{ns}	3.57	70.8
Asymmetry					
Obovoid	38.26***	7.30***	11.02*	2.53	40.89
Ovoid	18.82**	4.77***	14.96*	2.57	58.88
Asv	12.29^{ns}	0.04^{ns}	15.92^{ns}	2.25	69.5
Asob	25.29***	11.37***	11.82^{ns}	2.36	49.16
Asov	19.22**	5.97***	14.62*	3.41	56.78
Width_WP	33.22***	5.42***	13.20*	2.1	46.06
Internal Eccentricity					
Eccentricity	17.66**	10.98***	10.72^{ns}	3.73	56.91
P_Eccentricity	15.2^{ns}	0.00^{ns}	8.78^{ns}	6.91	69.11
D_Eccentricity	14.19^{ns}	0.18^{ns}	11.4^{ns}	5.75	68.48
F_Shape_I	46.1***	10.80***	19.86***	1.01	22.23
Ec_Area	39.85***	6.48***	22.98***	2.88	27.81

911 ***, **, *, ns indicate respectively, significant differences at p values <0.001, <0.01, and
912 <0.05 or not significative ($p \geq 0.05$).
913
914

Table 4. List of putative QTLs for the fruit shape traits analyzed found in the ILs and their physical position into the "67/3" eggplant reference genome, along with the increase over the recipient parent AN-S-26 and their allelic effects in the open field (OF) and screenhouse (SH).

Trait	QTL	Chr.	Physical position (Mb)	Ils carrying the QTL	Increase over AN-S-26 (%)		Allelic effect	
					OF	SH	OF	SH
Basic Measurements								
Width_Mh[a]	*wmh3*	3	93 - 96	SMI_3.6	32.09	25.78	0.64	0.54
	wmh10	10	0 -2	SMI_10.1	48.96	26.25	0.98	0.55
Max_Width[a]	*mw3*	3	93 - 96	SMI_3.6	31.64	25.52	0.65	0.56
	mw10	10	0 -2	SMI_10.1	48.6	23.85	1.00	0.52
Fruit Shape Index								
F_Shape_E_I[b]	*fseI2*	2	75 - 81	SMI_2.4	-15.17	-29.99	-0.12	-0.27
	fseI3	3	78 - 86	SMI_3.1, SMI_3.5	-7.79	-10.71	-0.06	-0.09
	fseI4	4	4 - 85	SMI_4.1, SMI_4.3	-13.01	-19.75	-0.11	-0.17
	fseI7	7	129 - 135	SMI_7.1, SMI_7.2, SMI_7.5	-18.44	-44.41	-0.15	-0.39
F_Shape_E_I[b]	*fseII2*	2	75 - 81	SMI_2.4	-13.8	-32.97	-0.11	-0.30

	fseII3	3	78 - 86	SMI_3.1, SMI_3.5	-6.66	-11.25	-0.06	-0.10
	fseII4	4	4 - 85	SMI_4.1, SMI_4.3	-13.63	-21.84	-0.11	-0.20
	fseII7	7	129 - 135	SMI_7.1, SMI_7.2, SMI_7.5	-18.95	-47.57	-0.16	-0.43
	cfs2	2	75 - 81	SMI_2.4	-13.31	-30.44	-0.11	-0.28
C_F_Shape[b]	*cfs3*	3	78 - 86	SMI_3.1, SMI_3.5	-7.80	-11.64	-0.07	-0.11
	cfs4	4	4 - 85	SMI_4.1, SMI_4.3	-13.81	-22.92	-0.12	-0.21
	cfs7	7	129 - 135	SMI_7.1, SMI_7.2, SMI_7.5	-19.12	-45.08	-0.16	-0.42
Blockiness								
P_Blockiness	*pfb1*	1	27 - 36	SMI_1.1, SMI_1.3	-15.45	-18.82	-0.05	-0.06
	pfb12	12	3 - 96	SMI_12.6	-11.45	-22.07	-0.03	-0.07
D_Blockiness	*dfb4*	4	4 - 85	SMI_4.1, SMI_4.3	-9.37	-16.31	-0.04	-0.06
	dfb8	8	3 - 109	SMI_8.1	-13.53	-17.13	-0.05	-0.07
Homogeneity								
Ellipsoid	*eli4*	4	4 - 85	SMI_4.1, SMI_4.3	-22.51	-39.17	-0.01	-0.01
	eli7	7	129 - 135	SMI_7.1, SMI_7.2, SMI_7.5	-33.82	-22.01	-0.01	-0.01
Circular[b]	*cir2*	2	75 - 81	SMI_2.4	-25.05	-54.96	-0.02	-0.05

	cir3	3	78 - 86	SMI_3.1, SMI_3.5	-14.08	-21.66	-0.01	-0.02
	cir4	4	4 - 85	SMI_4.1, SMI_4.3	-27.27	-42.00	-0.02	-0.04
	cir7	7	129 - 135	SMI_7.1, SMI_7.2, SMI_7.5	-41.40	-68.53	-0.03	-0.06
	rec1	1	27 - 36	SMI_1.1, SMI_1.3	-9.36	-6.55	-0.02	-0.02
	rec5	5	35 - 43	SMI_5.1	-6.30	-7.65	-0.02	-0.02
Rectangular	*rec10*	10	0 -2	SMI_10.1	-7.70	-7.79	-0.02	-0.02
	rec12	12	3 - 96	SMI_12.6	-10.16	-9.41	-0.03	-0.02
Asymmetry								
Obovoid	*obv8*	8	3 - 109	SMI_8.1	-35.75	-44.44	-0.04	-0.05
Internal Eccentricity								
	fsi2	2	75 - 81	SMI_2.4	-13.54	-31.78	-0.11	-0.28
	fsi3	3	78 - 86	SMI_3.1, SMI_3.5	-7.73	-10.54	-0.06	-0.09
F_Shape_I[b]	*fsi4*	4	4 - 85	SMI_4.1, SMI_4.3	-13.95	-20.82	-0.12	-0.19
	fsi7	7	129 - 135	SMI_7.1, SMI_7.2, SMI_7.5	-19.86	-46.44	-0.17	-0.42
	eca1	1	27 - 36	SMI_1.1, SMI_1.3	-4.40	-8.70	-0.01	-0.02
Ec_Area	*eca4*	4	4 - 85	SMI_4.1, SMI_4.3	-5.96	-8.58	-0.01	-0.02

eca8	8	3 - 109	SMI_8.1	-5.67	-8.11	-0.01	-0.02
eca9	9	5 - 34	SMI_9.1	-5.75	-8.85	-0.01	-0.02
eca10	10	0 -2	SMI_10.1	-4.94	-10.08	-0.01	-0.02
eca12	12	3 - 96	SMI_12.6	-4.16	-9.44	-0.01	-0.02

Table 5. Effect prediction on protein functionality using SIFT (cutoff = 0.05) and PROVEAN (cutoff = -2.5) software for the homozygous variants between the two parents of the IL population in eggplant genes identified as putative orthologous of tomato genes controlling fruit shape belonging to the SUN, OVATE and YABBY gene families. The ILs in which the allelic variant of the *S. incanum* donor parent MM577 is present in the background of the *S. melongena* recurrent parent MM577 are indicated for each gene. If not present in any of the ILs it is indicated by a minus (-) sign.

Gene	Eggplant locus	Variant type	aa Change	Parent alleles	SIFT		PROVEAN		ILs carrying the variant
					Predicted effect	Score	Predicted effect	Score	
SlSUN2	SMEL_001g148580.1	SNP	G317R	MM557	Deleterious	0.00	Neutral	0.618	SMI_1.1
		SNP	D331H	MM557	Deleterious	0.00	Neutral	-0.461	
		del_ins	P346S	MM557	Deleterious	0.00	Neutral	0.524	
SlSUN7	SMEL_002g164780.1	SNP	K26N	MM557	Deleterious	0.00	Neutral	-2.497	SMI_2.4
SlSUN10	SMEL_003g184300.1	SNP	S441N	MM557	Deleterious	0.00	Neutral	-0.545	SMI_3.1, SMI_3.5
SlSUN11	SMEL_003g197880.1	SNP	L285R	MM557	Deleterious	0.00	Neutral	-0.212	SMI_3.6
SlSUN13	SMEL_000g044110.1	SNP	F452S	AN-S-26	Deleterious	0.00	Neutral	0.360	-

SlSUN14	SMEL_004g221920.1	SNP	P140L	MM557	Deleterious	0.00	Neutral	0.203	SMI_4.1
		SNP	P458S	MM557	Deleterious	0.00	Neutral	0.397	
		SNP	K763N	MM557	Deleterious	0.00	Neutral	1.032	
SlSUN15	SMEL_010g349640.1	SNP	D521N	MM557	Neutral	0.07	Deleterious	-3.212	-
SlSUN16	SMEL_006g250960.1	SNP	A93V	MM557	Deleterious	0.00	Neutral	0.749	-
SlSUN19	SMEL_008g297530.1	SNP	S304L	MM557	Deleterious	0.00	Neutral	-1.228	-
		SNP	T352R	MM557	Deleterious	0.00	Neutral	1.839	
		SNP	M355L	MM557	Deleterious	0.00	Neutral	-0.417	
		SNP	S364N	MM557	Deleterious	0.00	Neutral	-0.939	
		SNP	C394G	MM557	Deleterious	0.00	Neutral	1.344	
SlSUN22	SMEL_008g305570.1	SNP	V12I	MM557	Deleterious	0.00	Neutral	0.010	SMI_8.1
		SNP	I297V	MM557	Deleterious	0.00	Neutral	0.353	
SlSUN23	SMEL_008g318520.1	SNP	N60T	MM557	Deleterious	0.00	Neutral	1.190	SMI_8.1
		SNP	R445G	MM557	Deleterious	0.00	Neutral	4.057	
SlSUN25	SMEL_009g322090.1	SNP	E235K	MM557	Neutral	0.86	Deleterious	-3.547	-
		SNP	Y242S	MM557	Neutral	0.71	Deleterious	-4.767	

SlSUN26	SMEL_009g331590.1	SNP	R20K	MM557	Deleterious	0.00	Neutral	0.367	SMI_9.1
		SNP	S77A	MM557	Deleterious	0.00	Neutral	0.411	
		ins	T123_A124insA	MM557	-	-	Neutral	1.722	
		SNP	E454Q	MM557	Deleterious	0.00	Neutral	0.306	
SlSUN31	SMEL_012g395480.1	SNP	L535W	MM557	Deleterious	0.00	Deleterious	-3.260	SMI_12.6
SlSUN32	SMEL_012g380740.1	SNP	C215F	MM557	Deleterious	0.00	Neutral	1.106	-
		SNP	S296A	MM557	Deleterious	0.00	Neutral	0.912	
SlOFP10	SMEL_005g229890.1	SNP	E162V	AN-S-26	Neutral	0.70	Deleterious	-5.967	-
SlOFP22	SMEL_010g357940.1	SNP	E240G	MM557	Neutral	0.43	Deleterious	-3.350	-
		SNP	M253I	MM557	Neutral	1.00	Deleterious	-3.500	
		SNP	Y274N	MM557	Neutral	0.85	Deleterious	-8.900	
SlYABBY2b	SMEL_012g395510.1	SNP	H169R	AN-S-26	Neutral	0.38	Deleterious	-6.206	SMI_12.6
YABBY1a	SMEL_001g131520.1	SNP	H9Q	MM557	Deleterious	0.00	Neutral	0.150	SMI_1.1

935

Figures

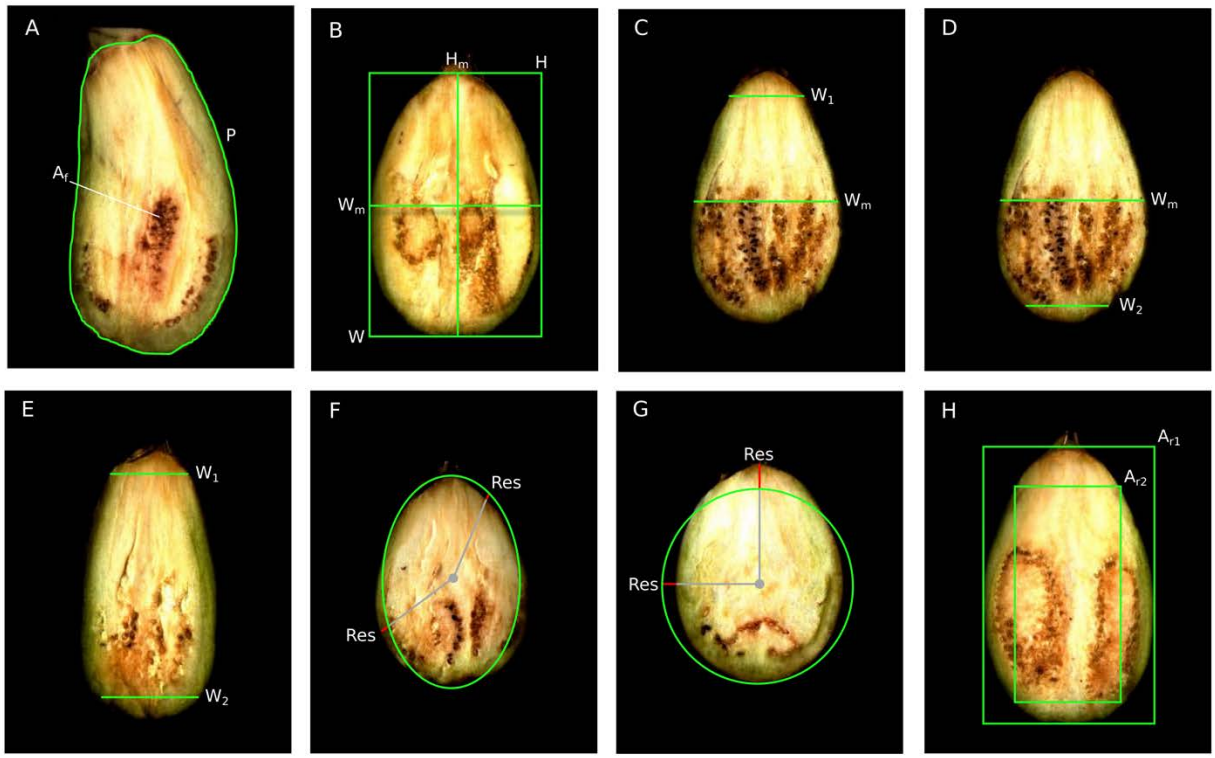

Figure 1. Visual representation of Tomato Analyzer descriptors used in this study and described in Table 1 using eggplant fruit. **A**) Perimeter (P) and fruit area (A_f). **B**) Fruit shape index external I, the ratio (H/W) of the maximum height (H) to maximum width (W), and Fruit shape index external II, the ratio (H_m/W_m) of height mid-width (W_m) to width mid-height (H_m). **C**) Proximal fruit blockiness, the ratio (W_1/W_m) of the width at the upper blockiness position (W_1) to width mid-height (W_m). **D**) Distal fruit blockiness, the ratio (W_2/W_m) of the width at the lower blockiness position (W_2) to width mid-height (W_m). **E**) Fruit shape triangle: the ratio (W_1/W_2) of the width at the upper blockiness position (W_1) to the width at the lower blockiness position W_2. **F**) Ellipsoid: the ratio of the error resulting from a best-fit ellipse to the area of the fruit. Error is the average magnitude of residuals (Res) along the fruit's perimeter, divided by the length of the major (longer) axis of the ellipse. **G**) Circular: the ratio of the error resulting from a best-fit circle to the area of the fruit. Error is the average magnitude of residuals along the fruit's perimeter, divided by the radius of the circle. **H**) Rectangular: the ratio of the area

(A_{r1}/A_{r2}) of the rectangle bounding the fruit (A_{r1}) to the area of the rectangle bounded by the fruit (A_{r2}). Further details on the descriptors are available at the Tomato Analyzer software webpage (https://vanderknaaplab.uga.edu/tomato_analyzer.html).

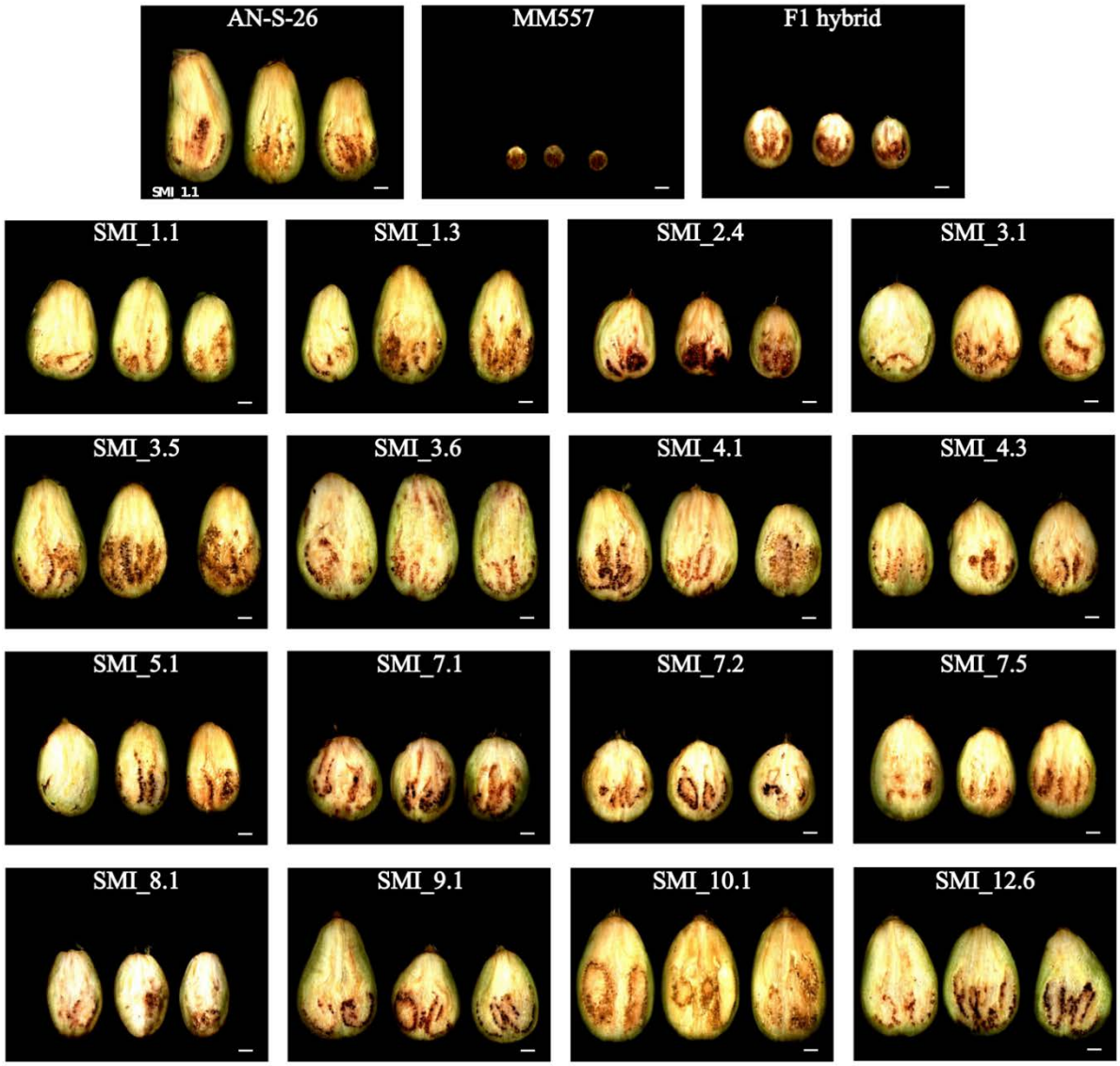

964

965 **Figure 2.** Representation of fruits scanned for the recipient parent (*S. melongena* AN-S-26),

966 donor parent (*S. incanum* MM577), their interspecific hybrid (F1 hybrid) and the 16 ILs used

967 in this study for the phenomic analysis and QTL detection for fruit shape.

968

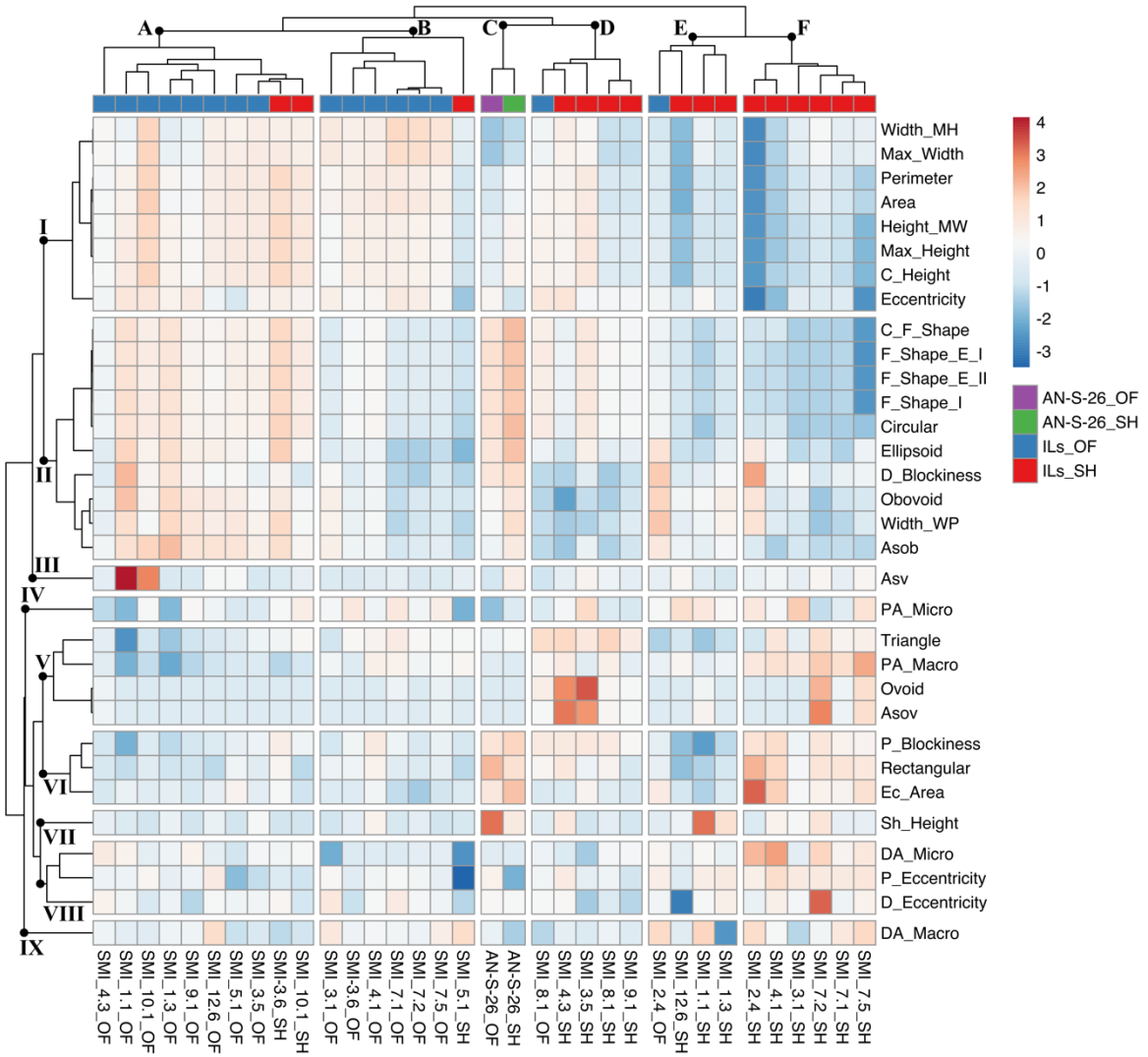

Figure 3. Hierarchical clustering heatmap for the recipient parent (AN-S-26) and the 16 ILs under open field (OF) and screenhouse (SH) conditions for the 32 Tomato Analyzer descriptors assessed in this study.

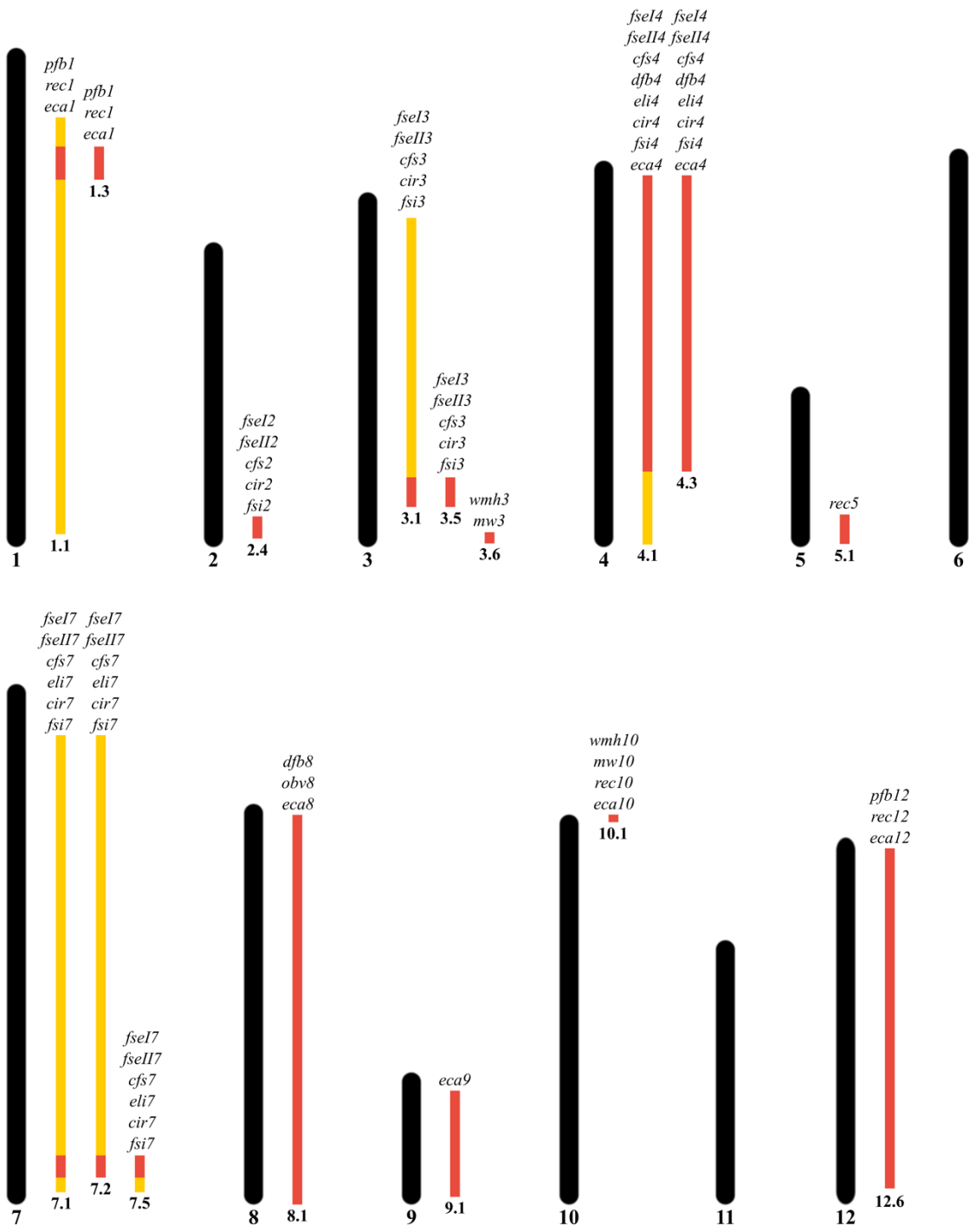

978

979 **Figure 4.** Physical position and size of the ILs (in yellow and/or red), compared to their

980 respective eggplant chromosomes (in black), and genomic regions carrying stable QTLs (in

981 red) identified in each line for the morphometric traits assessed with the phenomics tool

982 Tomato Analyzer. The name of the QTLs carried by each IL is indicated above the

983 corresponding IL, while an abbreviated QTL code (i.e., “1.1” stands for “SMI_1.1”) is
984 indicated below.
985